ORIGINAL PAPER



Mechanisms controlling persistent South Atlantic Convergence Zone events on intraseasonal timescales

Wendell M. B. Fialho¹ · Leila M. V. Carvalho² · Manoel A. Gan³ · Sandro F. Veiga⁴

Received: 16 March 2022 / Accepted: 13 January 2023 / Published online: 31 January 2023 © The Author(s), under exclusive licence to Springer-Verlag GmbH Austria, part of Springer Nature 2023

Abstract

The South Atlantic Convergence Zone (SACZ) is an important component of the South American Monsoon System. It is characterized by a persistent convective band with northwest-southeast orientation extending from tropical South America to Southwestern South Atlantic. The SACZ exhibits remarkable spatial and temporal variability and plays a critical role in regulating precipitation intensity and totals for millions of people living in South America. This study investigates mechanisms explaining persistent SACZ events (longer than 7 days) that often cause floods and landslides. This analysis extends from October 1996 to April 2014. To investigate the potential for subseasonal forecast of these events, this study focuses on mechanisms on intraseasonal timescales (20–90 days). We show that persistent SACZ events are preceded by a semi-stationary midlatitude Rossby wave train over the South Pacific with an equivalent barotropic structure that turns equatorward after crossing subtropical latitudes of South America. One distinctive feature of these events is the intensification of a trough in midlatitudes South Pacific westward of the Chilean coast preceding the events. Moreover, cyclonic persistent anomalies associated with the wave train over the western South Atlantic organize the oceanic SACZ six to 7 days before the events. Concomitantly, a persistent region with negative sea surface temperature (SST) anomalies emerges southward of the SACZ (between 30°S and 50°S) adjacent to the South American coast, likely resulting from the coupling between cyclonic circulation and the oceanic SACZ. Together, these processes strengthen the low-level westerlies on the SACZ equatorward side, causing the continental SACZ to intensify sustained by anomalous cyclonic circulation and enhanced southeastward moisture transport over land. Consequently, convection increases over the continent and the SACZ maintains active for long periods. Although shorter SACZ events (4 days) appear associated with the presence of a midlatitude wave train, their transient nature leads to distinct coupling effects. These observations are relevant for predicting long-lasting SACZ events.

Wendell M. B. Fialho wendell.fialho@inpe.br

Leila M. V. Carvalho leila@eri.ucsb.edu

Manoel A. Gan manoel.gan@inpe.br

Sandro F. Veiga sandroveiga@nju.edu.cn

- Center for Weather Forecasting and Climate Studies, The National Institute for Space Research, Cachoeira Paulista, SP 12630-000, Brazil
- Department of Geography and Earth Research Institute, University of California, Santa Barbara, Santa Barbara, CA 93106, USA
- Center for Weather Forecasting and Climate Studies, The National Institute for Space Research, São José Dos Campos, SP 12227-010, Brazil
- School of Atmospheric Sciences and Key Laboratory of Mesoscale Severe Weather, Ministry of Education, Nanjing University, Nanjing, China

1 Introduction

The South Atlantic Convergence Zone (SACZ) is a unique atmospheric feature of the South American monsoon system (SAMS). It is commonly defined as a band of convection and precipitation with a northwest-southeast orientation that remains stationary for a few days (Kodama 1992, 1993; Carvalho et al. 2002a, 2004). When active, the SACZ transports moisture from the tropics to subtropical latitudes and can cause precipitation over the southwestern South Atlantic (Carvalho et al. 2004, 2011; Pezzi et al. 2005, 2022). Thus, the SACZ and respective moisture transport modulates the seasonal precipitation cycle over tropical South America (Gan et al 2004; Vera et al. 2006; Silva and Carvalho 2007; Vasconcelos Junior et al. 2018) playing a significant role in water supply for millions of people.

Kodama (1993) recognized that the SACZ, like other subtropical convergence zones, is characterized by strong interactions between tropical moisture convergence and



extratropical dynamical forcing. It can be identified as an area of frontogenesis in equivalent potential temperatures and generation of convective instability. Thus, the SACZ exhibits great contrasts in moisture between its equatorward and poleward flanks. Geographically, the SACZ activity can extend from the central-southern Amazon to southeastern Brazil over land, eventually extending toward the southwest Atlantic Ocean (Quadro 1994; Carvalho et al. 2002a, 2004; Ferreira et al. 2004; Jorgetti et al. 2014).

However, Carvalho et al. (2002a, 2004, 2011) showed that the spatial characteristics of the SACZ are complex. These previous studies have shown the existence of two types of SACZ: continental SACZ and oceanic SACZ. These two types of SACZ may occur independently or may be connected. Carvalho et al. (2004, 2011) and Pezzi et al (2005, 2022) showed that distinct atmosphere-land—ocean coupling mechanisms drive the oceanic and continental SACZ. Also relevant, oceanic and continental SACZs play different roles in the spatial distribution of rainfall and extremes (Liebmann et al. 2001; Carvalho et al. 2002a).

The SACZ exhibits variations on subseasonal (Nogués-Paegle and Mo 1997; Liebmann et al. 1999; Herdies et al. 2002; Carvalho et al. 2004; Muza et al. 2009; Vera et al. 2018) and interannual (Liebmann et al. 2001; Carvalho et al. 2002a, 2004; Muza et al. 2009; Bombardi et al. 2014a, b) as well as long-term trends (Zilli et al. 2019, 2021). On interannual timescales, Carvalho et al. (2004) indicated that the El Niño Southern Oscillation (ENSO) warm phase modulates the number of occurrences of oceanic and continental SACZ events. Also relevant, previous studies have shown relationships between convective activity in the Atlantic intertropical convergence zone (ITCZ) and the SACZ on seasonal-to-interannual timescales (Garcia and Kayano 2010; 2011).

On intraseasonal timescales, the SACZ is characterized by a dipole of enhanced-suppressed precipitation over eastern (climatological position of the SACZ) and southeast South America (e.g., Nogués-Paegle and Mo 1997; Liebmann et al. 1999; Carvalho et al. 2011). The positive phase of the dipole is characterized by enhanced precipitation in the subtropics and weakened precipitation over the SACZ. Strong meridional transport of moisture from the Amazon to southeastern South America by the South American lowlevel jet (SALLJ) has been associated with this phase of the dipole (Vera et al. 2018; Montini et al. 2019). The opposite phase is characterized by enhanced moisture transport to southeastern Brazil along the SACZ and suppressed precipitation in the subtropics over southeastern South America (Nogués-Paegle and Mo 1997; Doyle and Barros 2002). The Madden-Julian Oscillation (MJO, Madden and Julian 1994) is the most prominent mode of intraseasonal variability modulating precipitation and their extremes in monsoon regions (Jones 2016; Grimm 2019). The MJO influences the active and break phases of the South American Monsoon (Jones and Carvalho 2002; Grimm et al. 2021) and the SACZ (Carvalho et al. 2004; Muza et al. 2009). Gonzalez and Vera (2014) and Vera et al. (2018) showed that convection related to the dipole on intraseasonal timescales (30-90 days) is strongly influenced by the MJO and respective Rossby wave activity in the extratropics. According to Mo and Higgins (1998), the Rossby wave train can be forced by the MJO convective activity. Cunningham and Cavalcanti (2006) investigated teleconnections between anomalous convective activity over Indonesia on intraseasonal timescales (scales 2–10 days and 30–90 days) and the SACZ position. They found that the propagation of frontal systems in the subtropics does not always result in the organization of the SACZ. Moreover, they suggested that the MJO is more important in modulating convection when the SACZ is displaced equatorward of its position. In contrast, planetary Rossby wave trains propagating along Austral midlatitudes are more important in modulating convection when the SACZ is located either poleward or at its climatological position. Moreover, there is compelling evidence that enhanced convective activity in the oceanic SACZ is linked to suppressed convection in the Atlantic ITCZ on intraseasonal timescales (period between 10 and 90 days), a mechanism explained by the propagation of midlatitude wave trains along the South Atlantic during these events (see Fig. 4c Carvalho et al. 2011).

While the absence of the SACZ for long periods has been linked to devastating droughts (Rodrigues et al. 2019; Nobre et al. 2016; Coelho et al. 2016), persistent SACZ events can lead to major rainfall-related disasters with significant socioeconomic impacts. Large urban centers with high population concentration and communities living in poor conditions and areas of landslide risk are particularly vulnerable to rainfall-related disasters. Barcellos et al. (2016) investigated the potential for meteorological systems to cause natural disasters and identified that 57% of the 35 catalogued disasters in Duque de Caxias, state of Rio de Janeiro (Brazil), were related to the SACZ. Two of these episodes were associated with the long persistence of SACZ events. One of them (from January 10 to January 20, 2004) resulted in 3 deaths and 1268 property losses. The November 12–26/2013 event resulted in major floods, 7000 property losses, and 2 deaths. Furthermore, persistent SACZ events can increase the chance of debris flow and landslides, particularly in coastal regions or areas with unstable steep terrain (Ferraz 2000). Two recent tragic events, on February 15/2022 when 258 mm were recorded in an interval of 4 h (4:20-7:00 PM LT), and on March 20/2022 when 415 mm of rain fell in just 10 h (217.4 mm of that total between 2:00 and 6:00 PM), led to flash floods and horrific mudslides affecting the mountainous city of Petropolis, state of Rio the Janeiro, Brazil (Alcântara et al. 2022). Both rainfall-related disasters, which



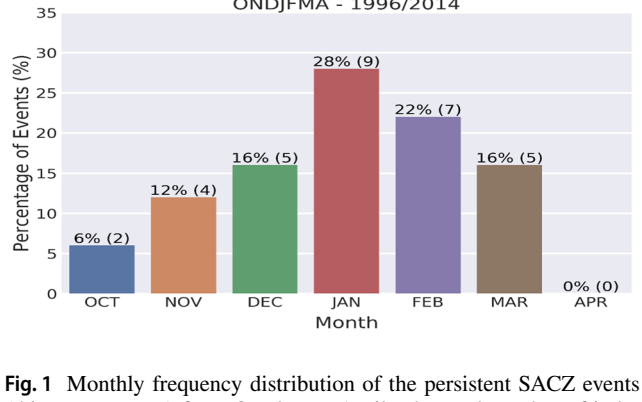
appeared related to the development of the oceanic SACZ, caused together over 238 fatalities (231 on February 15 and 7 on March 20) and millions of dollars in property losses.

The objective of this study is to understand atmospheric dynamical mechanisms influencing persistent SACZ events (persistence greater than 7 days) focusing on processes operating on intraseasonal timescales. For this purpose, we investigate atmospheric circulation and convection and examine underlying ocean-atmosphere coupled processes revealed in sea surface temperature (SST) anomalies on intraseasonal timescales. The stationary behavior of the SACZ exposes populated areas to rainfall-related hazards, being particularly dangerous for those living in coastal zones and regions with complex orography. In addition to advancing the present understanding of the SACZ, this study aims to provide simple "rules of thumb" to improve the capability of predicting persistent precipitation events with potential of causing floods and landslides, alleviating the impacts of these natural disasters to vulnerable communities. To achieve these goals, this article is organized as follows: datasets and methods are described in Section 2; the selection of SACZ cases, the band-filtering methodology, and statistical tests used in lag composites are presented in Section 3. The main results are discussed in Section 4, and conclusions and contributions to improve forecast of persistent SACZ events are presented in Section 5.

2 Data sets

One important objective of this study is to investigate SACZ events that have been catalogued based on criteria utilized in operational analyses developed at the Brazilian Center of Weather Forecast and Climatic Studies, National Institute of Space Research (CPTEC/INPE). Thus, episodes of

Fig. 2 Interannual variability of the persistent SACZ events from October to April. The respective number of events per season and the ENSO phases El Niño (EN), La Niña (LN), and neutral (N) are indicated at the top of the bars

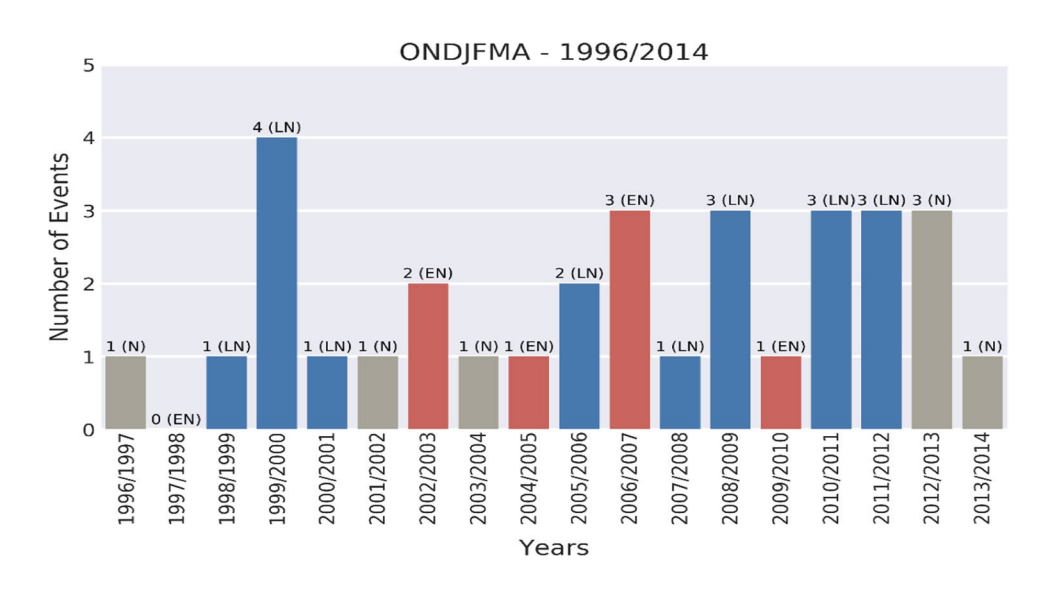


ONDJFMA - 1996/2014

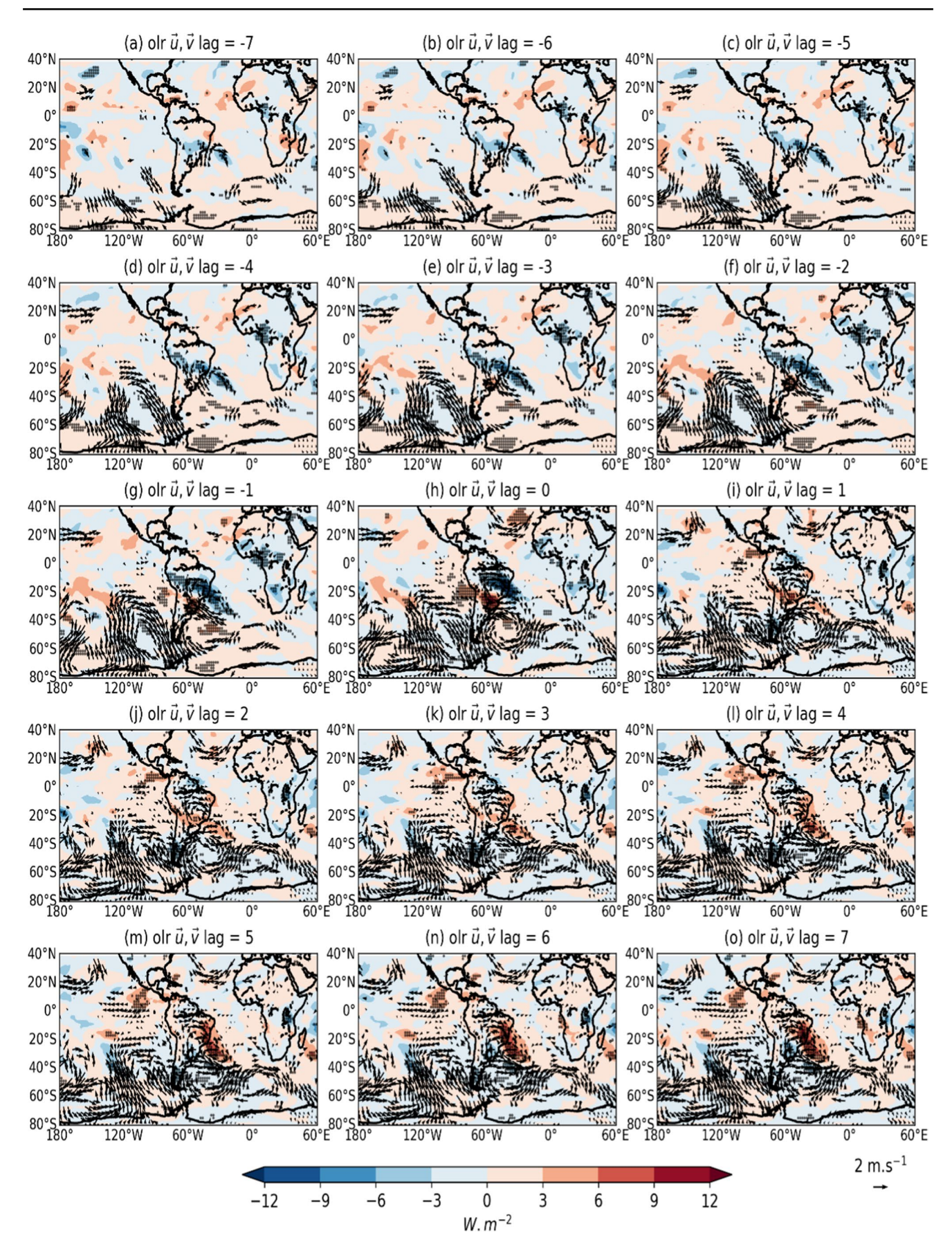
(thirty-two events) from October to April. The total number of independent events is shown in parentheses

SACZ events were compiled based on monthly reports from the Climanalise Bulletin, which are available from October 1996 to April 2014 (eighteen summers), and published by CPTEC/INPE. This data set is available at http://climanalise.cptec.inpe.br/~rclimanl/boletim/ and discussed in Rosso et al. (2018). These SACZ episodes were identified based following criteria: (1) persistent cloudiness (greater or equal than 4 days) based on brightness temperature; (2) moisture convergence at 850 hPa; (3) high potential temperature ($\theta_{\rm a}$) in midlevels of the atmosphere; (4) the presence of a trough at 500 hPa west of the region with maximum surface convergence; (5) organized ascending movement with northwest-southeast orientation in the middle troposphere: (6) anticyclonic vorticity and divergence in upper levels. These criteria are based on descriptions of the SACZ in Kodama (1992), Quadro (1994), Sanches (2002), and Ambrizzi and Ferraz (2015).

To examine dynamical mechanisms, this study utilizes daily atmospheric data from the National Centers for Environmental Prediction (NCEP) Climate Forecast System Reanalysis









◄Fig. 3 Lag composites of intraseasonal anomalies (20–90 days) of OLR (shaded) (W.m⁻²) and 850 hPa winds (vectors) (m.s⁻¹) for persistent SACZ events. Areas with statistically significant (at 95% confidence level) OLR anomalies are shown with stippling pattern. Only statistically significant winds are plotted (see "Section 3" for details)

(CFSR) (Saha et al. 2010). This reanalysis has demonstrated good performance in representing the South American climate and precipitation characteristics (e.g., Carvalho et al. 2012; Quadro et al. 2012; Bueno Repinaldo et al. 2015). The largescale atmospheric circulation is described in this study with 850 hPa and 200 hPa zonal and meridional winds (u,v). Both data sets have an original horizontal resolution of $0.5^{\circ} \times 0.5^{\circ}$. Additionally, to characterize large-scale aspects of tropical convection, we used daily Outgoing Longwave Radiation (OLR) $(W.m^{-2})$ at $1^{\circ} \times 1^{\circ}$ spatial resolution from the Climate Data Record Program (CDR). This product was chosen because of the ability to combine the accuracy of a satellite polar sensor with the high temporal resolution of a geostationary one (Lee et al. 2004). Daily SST (°C) was obtained from the National Oceanic and Atmospheric Administration (NOAA), from the Optimum Interpolation Sea Surface Temperature (OISST) at $0.25^{\circ} \times 0.25^{\circ}$ latitude-longitude (Reynolds et al. 2007). This dataset uses satellite measurements (Advanced Very-High-Resolution Radiometer—AVHRR) and in situ data from ships and buoys. Note that composites of circulation, OLR, and SST anomalies have been performed after a bilinear interpolation from the original resolutions to $2^{\circ} \times 2^{\circ}$.

To investigate the relationships between persistent SACZ events and the MJO, we utilized two indices that have been popularly employed (Kiladis et al. 2014): the OLR-based MJO Index (OMI) proposed in Kiladis et al. (2014) and the daily Real-Time Multivariate MJO (RMM) index proposed in Wheeler and Hendon (2004). OMI is constructed based on the projection of 20-96-day filtered OLR, including all eastward and westward wave numbers, onto the two daily spatial EOF (EOF-1 and EOF-2) patterns of 30-96-day eastward filtered OLR. Moreover, to identify the MJO events with OMI, in this study, we adopted the methodology proposed by Jones (2009). In this case, an MJO event was defined when (1) the phase angle between EOF1 and EOF2 systematically rotated anticlockwise, indicating eastward propagation; (2) the amplitude $(EOF1^2 + EOF2^2)^{0.5}$ was always larger than 0.35; (3) the mean amplitude during the event was larger than 0.9; and (4) the entire duration of the event lasted between 30 and 90 days.

The RMM index (Wheeler and Hendon 2004) employed here is based on the combined Empirical Orthogonal Function (EOF) of OLR and circulation (zonal winds in 850 hPa and 200 hPa). This index has been commonly utilized to investigate and monitor the MJO in real time, as the RMM does not include band-filtered data (Lafleur et al. 2015). In this case, an MJO was defined when the RMM amplitude

was greater or equal to 1.0. No other criteria were used to identify the cycle of the event. Precipitation anomalies during MJO phases were characterized using the Global Precipitation Climatology Project (GPCP) daily precipitation at $1^{\circ} \times 1^{\circ}$ latitude–longitude resolution. GPCP was employed as an independent variable that has not been utilized to obtain the MJO indices discussed here.

3 Methodology

SACZ events examined in this study were observed during Austral summer, between October and April (consistent with Silva and Carvalho 2007; Carvalho et al. 2011; Gan et al. 2004) and were further classified according to persistence. Notice that this catalogue does not separate between "continental" and "oceanic" SACZ (Carvalho et al. 2002a, 2004). Additionally, in these classifications, only SACZ events with persistence greater or equal to 4 days are recorded. This study investigates thirty-two SACZ events with persistence greater than 7 days (hereafter referred to as persistent SACZ) and twenty-three SACZ events with persistence of 4 days (hereafter SACZ_{4-days}) for comparison.

The main goal of this study is to investigate intraseasonal variations in the SACZ. Thus, anomalies in the meteorological fields were calculated by first removing linear trends and then the mean annual cycle. Daily anomalies were further band-filtered on intraseasonal timescales (20-90 days) using Fast Fourier Transform (FFT). The 20-90-day band interval was chosen to properly remove all signals on synoptic scales (Jones et al. 1998). Mechanisms were examined based on lag composites with respect to the date of the SACZ event (lag-0). Composites at lag-0 are calculated as mean values of variables during the entire period that the SACZ was considered active. Negative (positive) lags indicate days preceding (succeeding) the SACZ events. Statistical significance in lag composites was assessed by applying the t-student tests, considering each SACZ episode as an independent event; all statistical significances were estimated at a 95% confidence level. Winds were considered statistically significant when either the meridional or zonal component was statistically significant. Notice that variables analyzed in these composites are distinct (albeit not independent) from those utilized to identify the SACZ events described above.

4 Results and discussion

4.1 Seasonal and interannual variability of persistent SACZ

Figure 1 shows the monthly (October–April) percent of SACZ persistent events from 1996 to 2014. Interestingly,



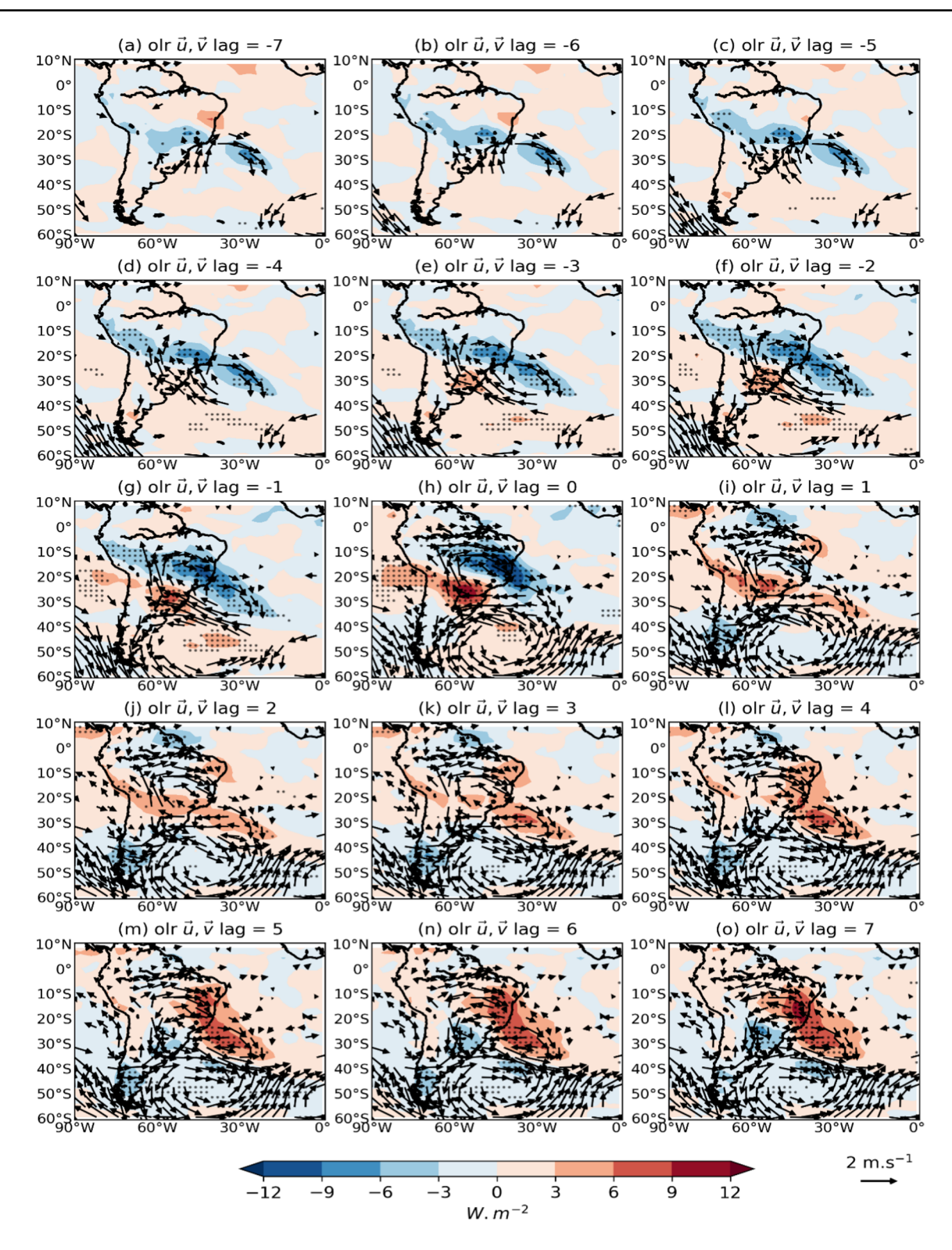


Fig. 4 Same as Fig. 3 but zoomed over South America

the distribution is not homogeneous throughout the monsoon season. Rather, the highest frequency of these events occurred in January (28%), followed by February (22%). This data set indicates that the total number of persistent events observed in January (nine) corresponds approximately to the total number of events observed in November (four) and December (five), suggesting that persistent SACZ events are more likely observed when the SAMS is well



established over South America (Carvalho et al. 2004; Gan et al. 2004; Silva and Carvalho 2007; Zilli and Hart 2021).

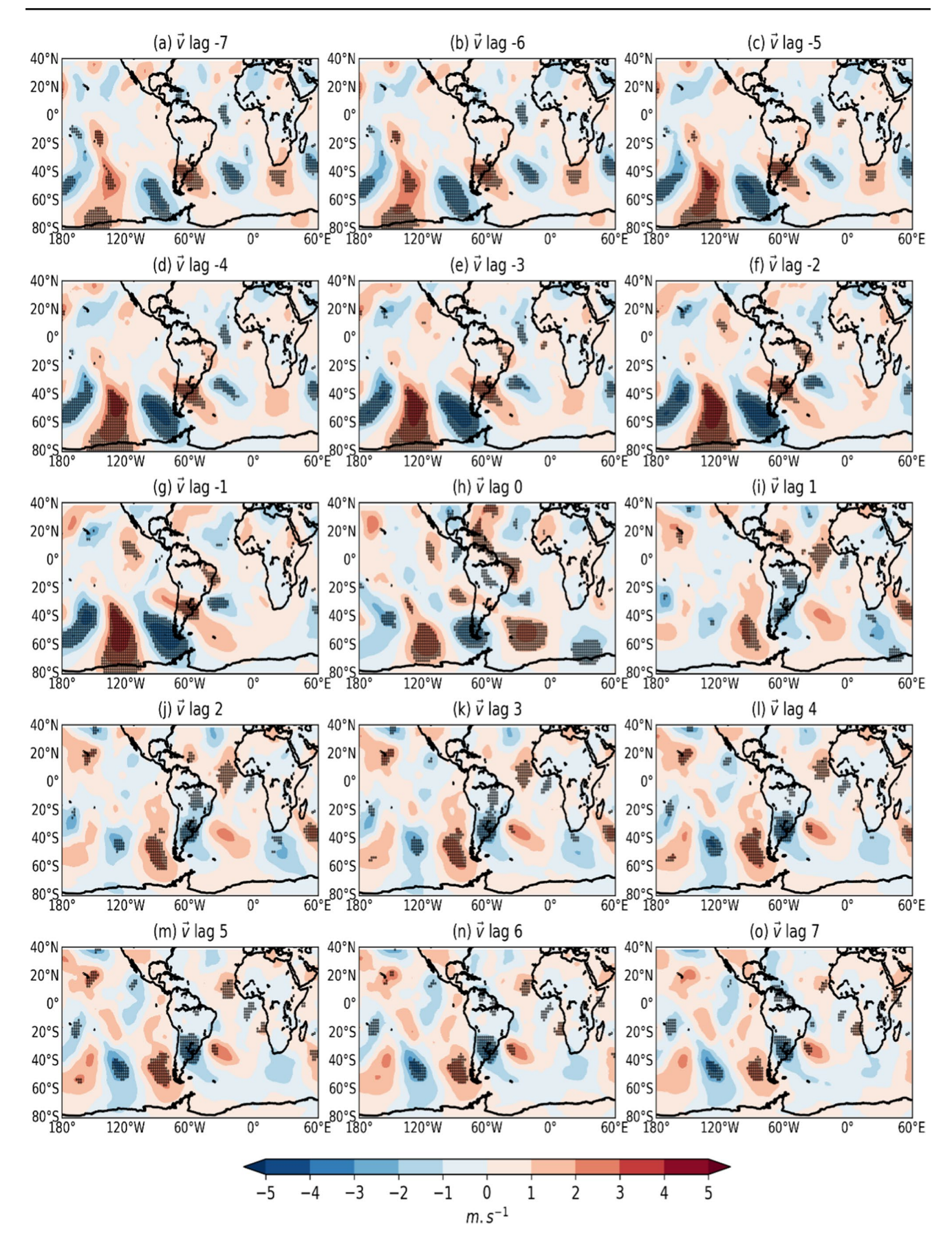
The interannual variability of the number of persistent SACZ events (between 1996 and 2014) is shown in Fig. 2. The ENSO is the most important mode of interannual variability affecting South America climate (e.g., Grimm et al. 2000). Here, we investigate the corresponding relationships between persistent SACZ and ENSO phases based on Niño-3.4 SST anomalies and the Oceanic Niño Index (ONI) (source: NCEP/Climate Prediction Center). During the analyzed period, we observe five El Niño (EN), eight La Niña (LN), and five neutral (N) years. ENSO phases are also indicated in Fig. 2. Although ENSO teleconnection patterns and relationships with convective variability over tropical South America depend on multiple factors and are seasonally dependent (e.g., Tedeschi et al. 2015; Grimm and Zilli 2009), previous studies have shown evidence that ENSO modulates the SACZ on interannual timescales (Liebmann et al. 2001; Carvalho et al. 2002a, 2004; Nieto-Ferreira et al. 2003; Ferreira et al. 2004). In this study, we have seven cases of SACZ during five EN (average of 1.4 events per season), eighteen during eight LN (average of 2.25 events per season), and seven during five neutral (average of 1.4 events per season) years. The maximum number of events (four) occurred in the LN season of 1999/2000. Despite the relatively small sample of ENSO phases, the z-test for the difference between two means (Spiegel and Stephens 1999) indicates that differences between LN and EN are statistically significant at a 90% confidence interval (p < 0.1) and LN and N are statistically significant at 94% confidence interval (p < 0.06). Although the relatively small sample size has influenced the statistical test, the increase in the frequency of the SACZ during the LN phase compared to the EN and N phases is consistent with previous observations. For instance, Carvalho et al. (2004) classified the SACZ according to continental and oceanic features and found that continental (oceanic) SACZs with persistence greater than 5 days are more frequent during LN (EN) events. As it will be shown, most of the persistent SACZ events investigated here, while preceded by oceanic SACZ, exhibited continental characteristics, which can explain the relatively stronger relationships with LN. Ferreira et al. (2004) have found a decrease in the number of SACZ events during EN years in 20 years of analysis and Nieto-Ferreira et al. (2003) showed enhanced SACZ during the 1999 LN year compared to the 1998 EN season. Nieto-Ferreira et al. (2003) findings are also consistent with our observation of the high frequency of SACZ persistent events in 1999 (Fig. 2). One possible mechanism of teleconnection between ENSO and the SACZ is the ENSO influence on the frequency and intensity of the SALLJ, which is another important component of the South American climate (Marengo et al. 2009). The SALLJ is critical in transporting moisture from the tropics to the subtropics during the summer monsoon, causing the weakening of the SACZ activity (Liebmann et al. 2004; Carvalho and Silva Dias 2021). Montini et al. (2019) demonstrated that the SALLJ is more frequent during EN compared to LN and neutral years, which could explain the weakening of the continental SACZ and the less frequent persistent SACZ events during EN, the opposite occurring during LN. Nevertheless, further studies with more case studies are necessary to obtain more robust statistics, and to further understand the relationships between persistent SACZ and ENSO.

4.2 Dynamical atmospheric mechanisms

To understand the spatial structure and dynamical mechanisms associated with the organization and evolution of persistent SACZ events, we examined lag composites of daily intraseasonal anomalies (20-90 days). We recall that lag-0 corresponds to the period when the SACZ is active over the continent; negative (positive) lags indicate days preceding (succeeding) the SACZ episode. Figure 3 shows lag composites of OLR (shaded) and 850 hPa winds 7 days preceding the events until 7 days after the events. Figure 4 shows the same lag composites as Fig. 3 but zoomed over South America and the western South Atlantic to better visualize anomalous circulation and OLR anomalies. Notice that the band-filtering (20–90 days) of the data sets results in small changes in the magnitude of circulation and OLR anomalies between consecutive lags. The starting of these analyses 7 days prior to the event was based on observations that anomalies were weak for longer lags (not shown). One remarkable signature of the organization of the SACZ that has been extensively shown in previous literature (e.g., Liebmann et al. 1999; Nogués-Paegle and Mo 1997; Nogués-Paegle et al. 2000; Carvalho et al. 2004; Cunningham and Cavalcanti 2006; Muza et al. 2009; Vera et al. 2018) is the association of these events with the organization of a midlatitude Rossby wave train. These wave trains, which exhibit an equivalent barotropic structure across the western South Pacific, reach South America and deflect northward over the South Atlantic basin after crossing the southern portion of the continent. In this study, we show that this wave train on intraseasonal timescales remains semi-stationary and intensifies over time, from lag -7 to lag -1 (Fig. 3), modifying circulation over tropical South America and favoring persistent SACZ events.

Seven days preceding the SACZ events (Figs. 3 and 4, lag -7 days), as part of the wave train pattern, an anomalous cyclonic circulation in 850 hPa is already evident off the coast of southeastern Brazil. This feature enhances







∢Fig. 5 Lag composites of 200 hPa meridional winds intraseasonal (20–90 days) anomalies (m/s) for persistent SACZ events. Only statistically significant anomalies (at 95% confidence level) are shown

convective activity over the ocean, inducing the oceanic SACZ from lag -7 to lag -1 (Carvalho et al. 2002a, 2004; Pezzi et al. 2022). On lag -4 days (Figs. 3 and 4), anomalous westerly winds intensify over tropical Brazil under the influence of the oceanic cyclonic circulation. Westerly wind anomalies further enhance moisture transport from the Amazon toward southeastern South America, increasing instability and convection over southeastern South America from lags -4 to -1 days; these results support the findings of previous studies (Carvalho et al. 2002b, 2004, 2011; Jones and Carvalho 2002; Rickenbach et al. 2002; Herdies et al. 2002; Muza et al. 2009; Marengo et al. 2009). Concomitantly, the Rossby midlatitude wave train intensifies in the extratropics over the Southern Ocean east of Chile, while maintaining its structure and stationary behavior (Fig. 3, lags -3 to -2 days). As convection enhances on lag -3 over southeastern Brazil (Figs. 3 and 4), suppressed convection is observed over southern Brazil and Uruguay, where the 850 hPa winds transport cooler and more stable air inland from the subtropical South Atlantic Ocean on the poleward flank of the oceanic SACZ.

On lag -1, the anomalous cyclonic center begins to shift from the ocean toward the continent, possibly driven by enhanced convection and latent heat feedback (e.g., Tao et al. 2001). This continental shift in the cyclonic anomalies further enhances westerly anomalies over tropical South America. The intensification in the 850 hPa westerly winds increases moisture transport and moisture transport convergence equatorward of the SACZ, intensifying the continental SACZ on lag-0 (Neelin and Held 1987; Schiro et al. 2016; Carvalho et al. 2011). The suppressed convection over southern Brazil and Uruguay (Fig. 4) appears related to the intensification of an anticyclonic anomaly poleward of the SACZ and difluence of the winds. On lag-0, convection is well developed over the continent in the climatological position of the continental SACZ (Carvalho et al. 2002a, 2004). Moreover, on lag-0, the anomalous anticyclone strengthens over subtropical South America in the southern flank of the SACZ, and a much broader region with suppressed convection extends over Northeastern Argentina, Paraguay, Uruguay, and Southern Brazil (Fig. 4). This seesaw in convective activity on intraseasonal timescales has been shown to be a remarkable feature associated with the SACZ (e.g., Nogués-Paegle and Mo 1997; Liebmann et al. 1999; Carvalho et al. 2011; Cunningham and Cavalcanti 2006; Vera et al. 2018). The midlatitude wave train pattern on intraseasonal timescales shown in this work resembles the Pacific-South American (PSA) pattern discussed in Nogués-Paegle et al. (2000).

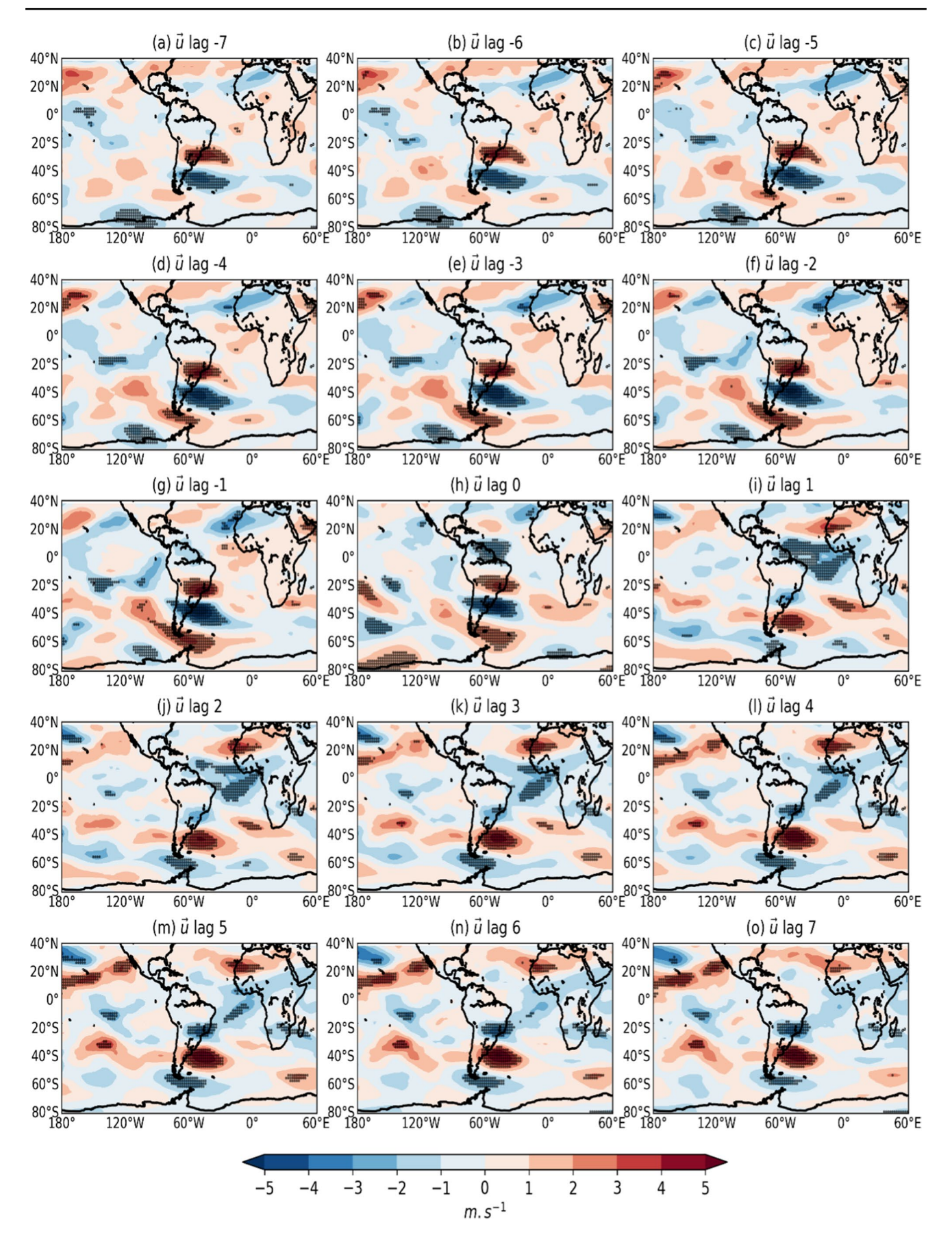
From lag + 1 to lag + 4 days, the cyclonic anomaly over tropical eastern South America weakens and is replaced by strong anticyclonic anomalies, with easterly winds transporting stable air from ocean to land, suppressing convection in the region where the SACZ was active in lag-0. The association between easterly wind anomalies and suppressed convection over tropical South America has been extensively demonstrated before (e.g., Carvalho et al. 2002b, 2004; Herdies et al. 2002; Jones and Carvalho 2002; Petersen et al. 2002). From lags + 5 to + 7 days, suppression (convection) dominates over southeastern (southern) Brazil (Fig. 4), reversing the signal of the seesaw, consistent with previous observations (e.g., Gonzalez and Vera 2014; Cunningham and Cavalcanti 2006; Gelbrecht et al. 2018).

The upper-level support for the organization of the SACZ is shown with lag composites of intraseasonal anomalies of the meridional (Fig. 5) and zonal winds (Fig. 6) at 200 hPa. Here, we separate both components to clarify and better characterize the midlatitude Rossby wave path. Composites of 200 hPa winds (u,v) and OLR anomalies can be seen in Supplemental Figs. S1 and S2.

Figure 5 illustrates the amplification of the midlatitude Rossby wave train and the relevance of monitoring the behavior of 200 hPa meridional anomalies as a potential predictor for persistent SACZ episodes. Of particular importance is the intensification of 200 hPa meridional wind anomalies over Southern Pacific, west of South America, as the Rossby wave train maintains its stationary behavior from lag -7 to lag -1. These anomalies are associated with the amplification of a trough west of South America (Fig. 5 and Supplemental Fig. S2). The strongest meridional anomalies in midlatitudes are observed between -2 and -1 days preceding the events. Meanwhile, the anticyclonic feature east of the Andes remains stationary with similar strength, as indicated by the southerly wind anomalies in the subtropics, blocking the eastward propagation of the Rossby wave until lag -1. On lag-0, 200 hPa meridional wind anomalies weaken over the eastern South Pacific (west of South America) and subtropical South America. The Rossby wave train then bifurcates in midlatitudes, with one path observed along eastern South America over the tropical South Atlantic Ocean, and the other path observed along the extratropical Atlantic following wave guides discussed in Hoskins and Ambrizzi (1993). Thus, the onset of a persistent SACZ event over the continent, while preceded by a stationary troughridge pair in midlatitudes across South America, is observed when the wave train intensifies eastern of South America and over the extratropical South Atlantic (Fig. 5 and Supplemental Fig. S2).

When the SACZ is active (lag-0), southerly (northerly) anomalies enhance equatorward (poleward) of the SACZ OLR anomalies (see Figs. 3 and 4) at 200 hPa (Fig. 5). These patterns indicate increased upper-level divergence associated







◄Fig. 6 Lag composites of 200 hPa zonal winds intraseasonal (20–90 days) anomalies (m/s) for persistent SACZ events. Only statistically significant anomalies (at 95% confidence level) are shown

with enhanced convection that induce cross-equatorial southerly winds (see Supplemental Figs. S1 and S2 for further details). This pattern of anomalies has been identified by Tomaziello et al. (2016) in association with intraseasonal anomalies in the trade winds and in the ITCZ. These observations also corroborate with the "increased upper-level divergence" and "anticyclonic circulation in upper-level" criteria utilized to identify SACZ events used here.

For lags following the SACZ event, the 200 hPa meridional winds anomalies (Fig. 5) clearly indicate a change in the phase of the wave train over tropical and subtropical South America, which is accompanied by changes in low-level winds favoring suppressed convection collocated with the position of the SACZ in lag-0 (Fig. 3).

Figure 6 complements the characterization of the upperlevel support for the development of persistent SACZ by showing intraseasonal anomalies of 200 hPa zonal winds. While 200 hPa meridional winds are relevant in monitoring the amplification of the wave train in midlatitudes across South America (Fig. 5), zonal winds in 200 hPa further characterize the presence of an anomalous stationary cyclonic vortex on the southern flank of the SACZ position. This feature persists from lag -7 to lag-0. The enhanced westerly winds in the subtropics (around 20°S) induce divergence aloft on the poleward exit of the upper-level jet. This region is colocated with convective activity observed over the oceanic SACZ prior to the development of the continental SACZ. These results reinforce the importance of the semi-stationary Rossby wave train in enhancing convection over the subtropical Atlantic prior to the development of convection over tropical South America. When the SACZ is active (lag-0) over the continent, we observe an anticyclonic circulation associated with the development of deep convection (Figs. 3 and 5, Supplemental S1), consistent with Kodama (1993), Carvalho et al. (2002a), Muza et al. (2009), and Bombardi et al. (2014b). At this stage, the wave train exhibits a baroclinic structure in the tropics where convection is enhanced (compare Fig. 4 and S2).

4.3 Persistent SACZ and South Atlantic SST anomalies

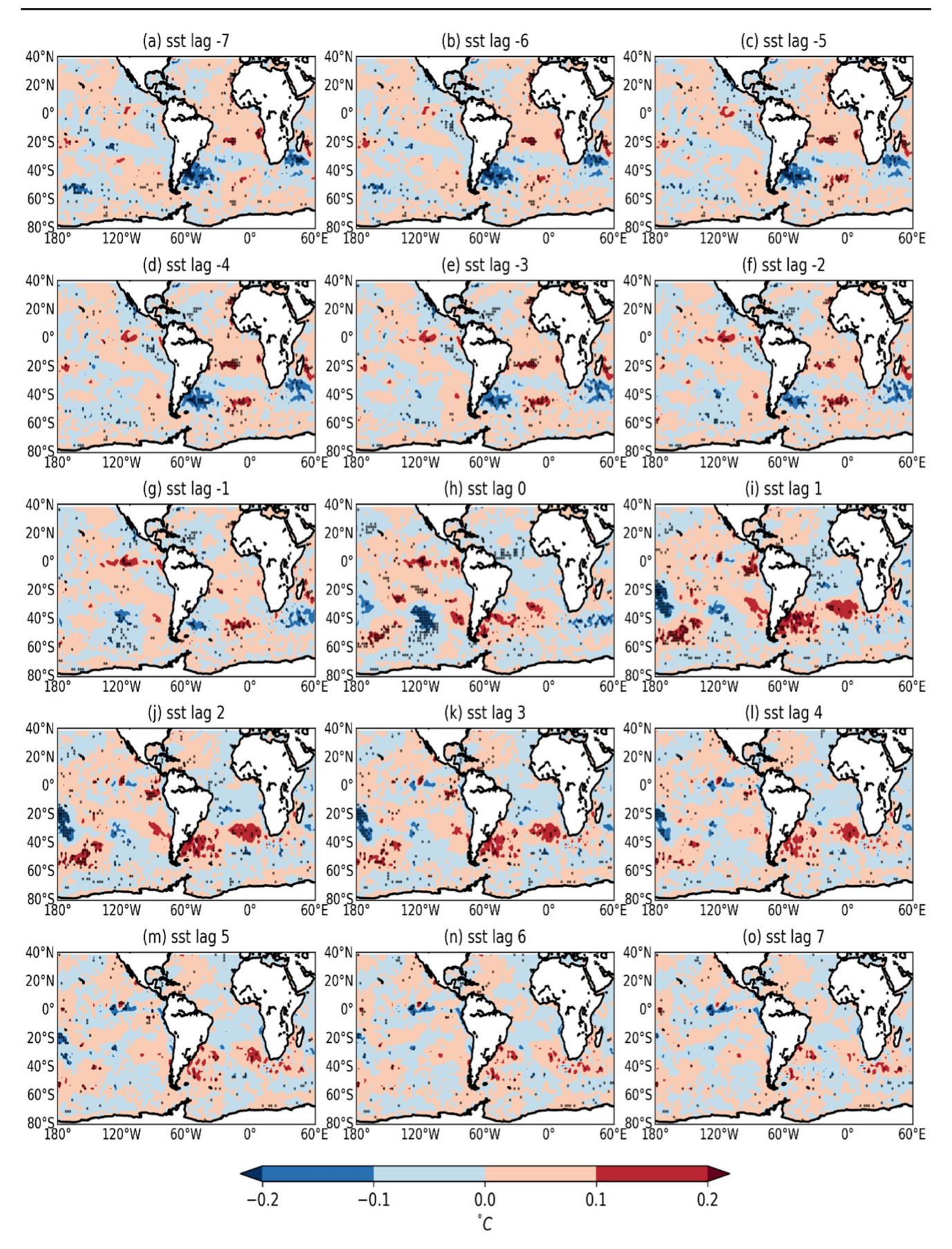
The coupling between the SACZ and SST anomalies has been investigated before on multiple spatiotemporal scales (e.g., Chaves and Nobre 2004; De Almeida et al. 2007; Bombardi et al. 2014a, b; Barreiro et al. 2002, 2005; Tirabassi et al. 2015; Pezzi et al. 2005, 2022). Here, consistently with our previous analyses, we investigate these relationships with lag composites of intraseasonal (20–90 days)

SST anomalies (Fig. 7). A remarkable feature emerging from these composites is the "blob" of cold SST anomalies adjacent to South America persisting from lag -7 until lag -1. Interestingly, from lag-0 to lag+4 days, these anomalies reverse sign and become positive. Pezzi et al. (2022) investigated the relationships between the oceanic SACZ and the Atlantic SST and proposed two distinct coupling mechanisms: thermodynamic and dynamic. The thermodynamic mechanism accounts for the direct impact of cloudiness and precipitation on the incoming short-wave radiation that results in the cooling of SST (e.g., Chaves and Nobre 2004; De Almeida et al. 2007). The dynamic mechanism, according to Pezzi et al. (2022), is a more complex type of coupling and involves interactions between winds and the oceanic boundary layer.

The blob of negative SST anomalies preceding the stationary SACZ (Fig. 7) is observed in a region that is influenced by the Brazil-Malvinas Confluence (BMC). The BMC is characterized by the convergence of two opposing western boundary currents: the tropical warm and saline waters transported by the Brazil Current from the north and the cold and less saline Sub-Antarctic waters transported by the Malvinas Current from the south (Peterson and Stramma 1991). Observational studies (Pezzi et al. 2005) have shown great contrasts in temperature and heat fluxes between the warm and cold sides of the BMC, showing evidence that synoptic systems can modulate SST differences due to strong near-surface winds. In a subsequent study, Acevedo et al. (2010) investigated changes in the atmospheric boundary layer in the BMC region caused by passages of frontal systems during October-November. They observed distinct behaviors in the cold and warm sides of the confluence, with the cold side exhibiting a more stably stratified boundary layer. Our lag composites suggest that the semi-stationary cyclonic center is positioned such that the respective southeasterly wind anomalies interact with the BMC (compare Fig. 3 with Fig. 1 in Acevedo et al. 2010). These winds may induce persistent cold air advection in the region and perturb the structure of the BMC, which could result in the observed negative pool of SST anomalies (Fig. 7). A stably stratified cool atmospheric boundary layer forms over the cold SST anomalies inhibiting convection (Acevedo et al. 2010) while increasing pressure gradient contrasts due to air masses with distinct thermodynamic characteristics (Pezzi et al. 2005). These gradients could contribute to maintaining the cyclonic anomaly over the subtropical South Atlantic, and consequently an active and stationary oceanic SACZ from lag -7 to lag -1 days (Figs. 3, 4, and 7).

On lag-0, when convection becomes more intense over land and cyclonic anomalies shift from the Atlantic to the continent, the blob with negative SST anomalies along the MBC is dismantled. An anticyclonic anomaly is now observed affecting the confluence region, possibly advecting







◄Fig. 7 Lag composites of SST intraseasonal anomalies (20–90 days) (°C) for persistent SACZ events. Statistically significant regions (at 95% significance level) are shown with stippled patterns

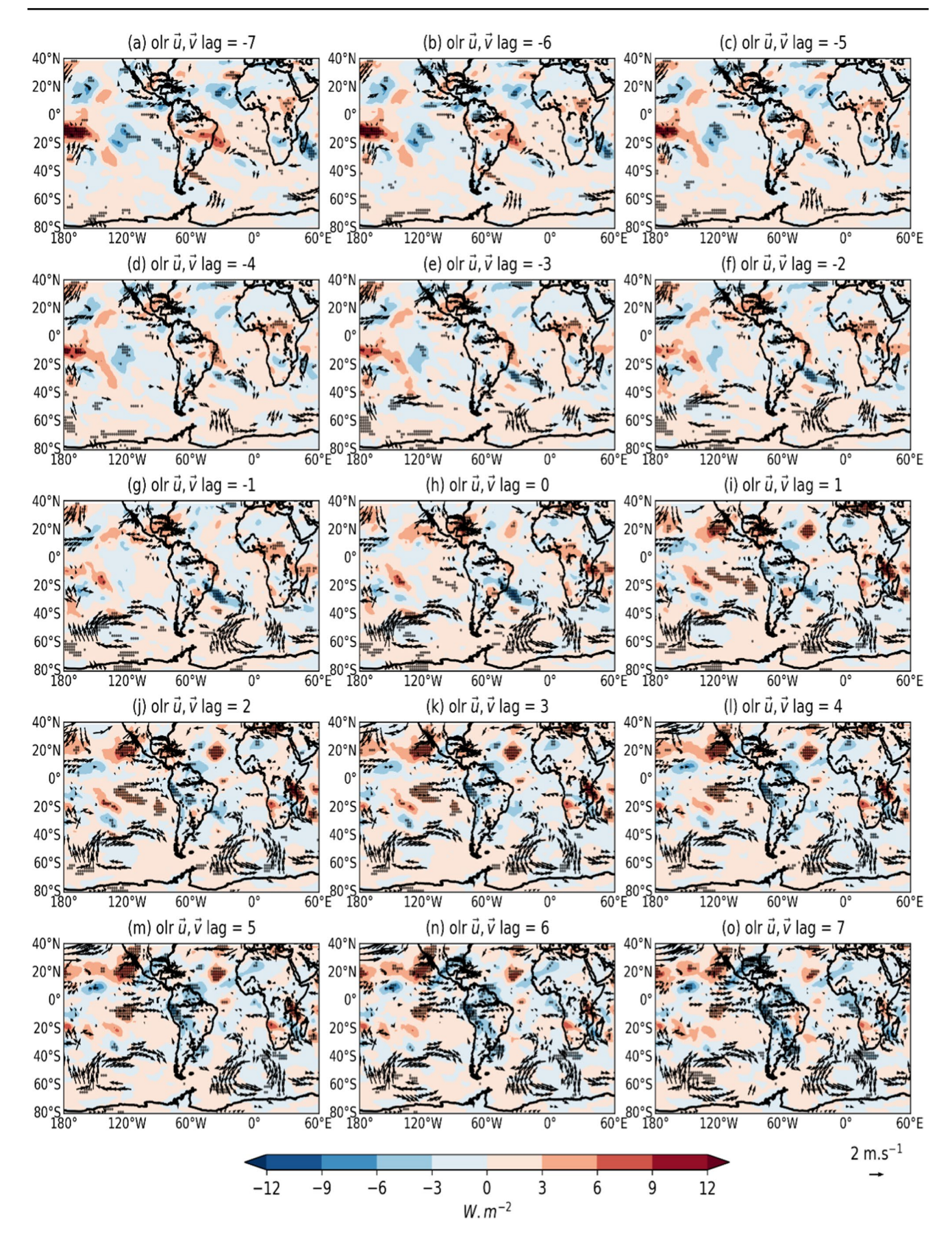
warmer water to the subtropics (Figs. 3 and 4). This process can explain the transition to a warm anomaly in the same region from lag-0 to lag+4 days. Therefore, these results indicate that the "dynamic" coupling mechanism dominates on intraseasonal timescales. Note that, except for a few statistically significant grid points, no negative SST anomalies are observed where the oceanic SACZ is active as should be expected according to the "thermodynamic" mechanism (i.e., negative feedback between the SACZ cloud cover inducing a reduction in short-wave radiation) proposed in Chaves and Nobre (2004). One possible reason for this discrepancy is the spatiotemporal scale investigated here. It is possible that cloud-short-wave feedback is a more transient (mesoscale) process (Pezzi et al. 2022) observed at scales that have been filtered in this study. Interestingly, we note that the cooling of the Subtropical South Atlantic shown here (Fig. 7) and hypothesized to be associated with perturbations in the BMC contrasts with results shown in Bombardi et al. (2014b). In that study, enhanced precipitation over the continent over Southeastern Brazil (the climatological position of the SACZ region) appeared related to the negative phase of the South Atlantic Dipole, characterized by warm temperatures in the subtropics and cold temperatures in the tropics. Therefore, stationary SACZ events seem to have a unique signature concerning South Atlantic SST anomalies. This implies that SST anomalies in the BMC are important to be monitored along with atmospheric circulation anomalies associated with the Rossby wave train in order to better predict the probability of persistent SACZ events.

4.4 Contrasting characteristics of short-lived SACZ events

To further evaluate the potential for discerning prognostics between long persistent SACZ events and relatively short events, we investigated circulation, OLR, and SST anomalies for twenty-three cases of SACZ_{4-days}. Notice that the Climanalise Bulletin does not include shorter-duration events. Figure 8 depicts 850 hPa anomaly winds and OLR, similar to Fig. 3, but for $SACZ_{4-days}$. While $SACZ_{4-days}$ appeared related to the presence of a Rossby midlatitude wave train, one remarkable difference between SACZ_{4-days} and persistent SACZ events is the less coherent pattern of wind anomalies around extratropical South America, possibly driven by the more transient nature of these events, indicating the importance of the synoptic scale anomalies filtered out in these analyses and greater case-to-case differences. Another interesting observation regards the configuration of the midlatitude wave trains between 40°S-60°S across South America (see Supplemental Fig. S3 for further details). Although the equivalent barotropic structure in midlatitudes is shared in both cases (not shown), across South America (i.e., between 180°W and 60°E), we observe a wavenumber-3 for SACZ persistent cases (Fig. 3) and wavenumber-1 for SACZ_{4-days}, with a semi-stationary pair trough-ridge on the eastern and western sides of Southern South America, respectively, from lag -3 to lag +4 (Fig. 8). Moreover, the $SACZ_{4-days}$ events exhibit also a distinct pattern of convective activity. First, the oceanic- SACZ_{4-days} appear to develop much far from the coast compared to persistent SACZs. The "embryo" oceanic-SACZ_{4-days} begins to develop on lag -7 in association with an anomalous cyclonic circulation around 30°S in the middle of the South Atlantic Ocean. This anomalous cyclone persists from lag -7 to lag +7 (Fig. 8). Noticeable, even during lag-0, the anomalous cyclonic circulation in the SACZ_{4-days} cases is not displaced over the continent, as observed during persistent SACZs (compare Fig. 3 lag-0 and Fig. 8 lag-0). Moreover, SACZ_{4-days} convection remains intense over the ocean on lag-0, contrasting with persistent SACZs. Also, there is no intensification of meridional winds in midlatitudes at 200 hPa during SACZ_{4-days} cases (not shown), despite the fact that the midlatitude cycloneanticyclone pair maintains stationary from lag -5 to lag +7 across South America. These observations indicate that persistent SACZs are driven by much stronger local and remote forcings and feedbacks comparatively to SACZ_{4-days}. More importantly, these differences can be clearly distinguished in lag composites of circulation and OLR.

Another remarkable difference between persistent SACZ and SACZ_{4-days} concerns SST anomalies (Fig. 9). Interestingly, anomalous features are observed during SACZ_{4-days} events that dramatically contrast with persistent SACZ. First, over the central South Atlantic, the persistent lowlevel cyclonic circulation appears to play a critical role in inducing SST anomalies over the South Atlantic Basin away from the continent. We hypothesize that, on the equatorward sector of the persistent anomalous cyclone, the westerly anomalies transport the relatively warm water of the Brazilian current eastward, whereas on the poleward sector of the cyclone, the easterly anomalies transport cold water from the Benguela current westward. These anomalous transports create the dipolar pattern of warm-cold SST anomalies over the subtropical South Atlantic (Fig. 9) from lag -7 to lag + 7. Also important, the cool pole of the dipolar feature seems partially overlaid by OLR negative anomalies associated with an oceanic SACZ from lag -5 to lag + 2 (compare Fig. 9 with Fig. 7). This indicates that the thermodynamic effect (i.e., cooling due to precipitation and cloudiness shortwave feedback— Chaves and Nobre 2004; Nobre et al. 2012; Pezzi et al. 2022) may also be present from lag -5 to lag +2. Nonetheless, from lag + 3 to lag + 7, the dipolar SST anomaly is maintained despite the absence of an oceanic SACZ,







√Fig. 8 Lag composites of intraseasonal anomalies (20–90 days) of OLR (shaded) (W.m⁻²) and 850 hPa winds (vectors) (m.s.⁻¹) for SACZ_{4-days} events. Areas with statistically significant (at 95% confidence level) OLR anomalies are shown with stippling pattern. Only statistically significant winds are plotted (see methods for details)

indicating that the dynamical mechanism (wind forcing) is critical in explaining these anomalies (Pezzi et al. 2022). Because the cyclonic anomaly is displaced eastward for SACZ_{4-days} compared to persistent SACZs, a similar dipolar structure over the central South Atlantic is not evident for persistent SACZs (compare Figs. 8 and 6). Furthermore, another interesting observation is that the SACZ_{4-days} events are associated with warm anomalies at the BMC region from lag -7 to lag +7, remarkably contrasting with persistent SACZs. We hypothesize that these anomalies result from the persistent anomalous anticyclonic circulation feature associated with the midlatitude wave trains on the east side of South America that would increase the transport of warm waters poleward by the Brazil current (Fig. 8).

4.5 Relationships between persistent SACZ and the MJO

Here, we investigate relationships between the MJO and persistent SACZ events to answer the specific question: does the probability of persistent SACZ events significantly increase when the MJO is active? Furthermore, a comparison among MJO indices by Kiladis et al. (2014) indicated that different indices may lead to different results. Therefore, we also aim to answer the following question: is the relationship between persistent SACZ events and the MJO sensitive to the employed MJO index and methodology to define the MJO cycle?

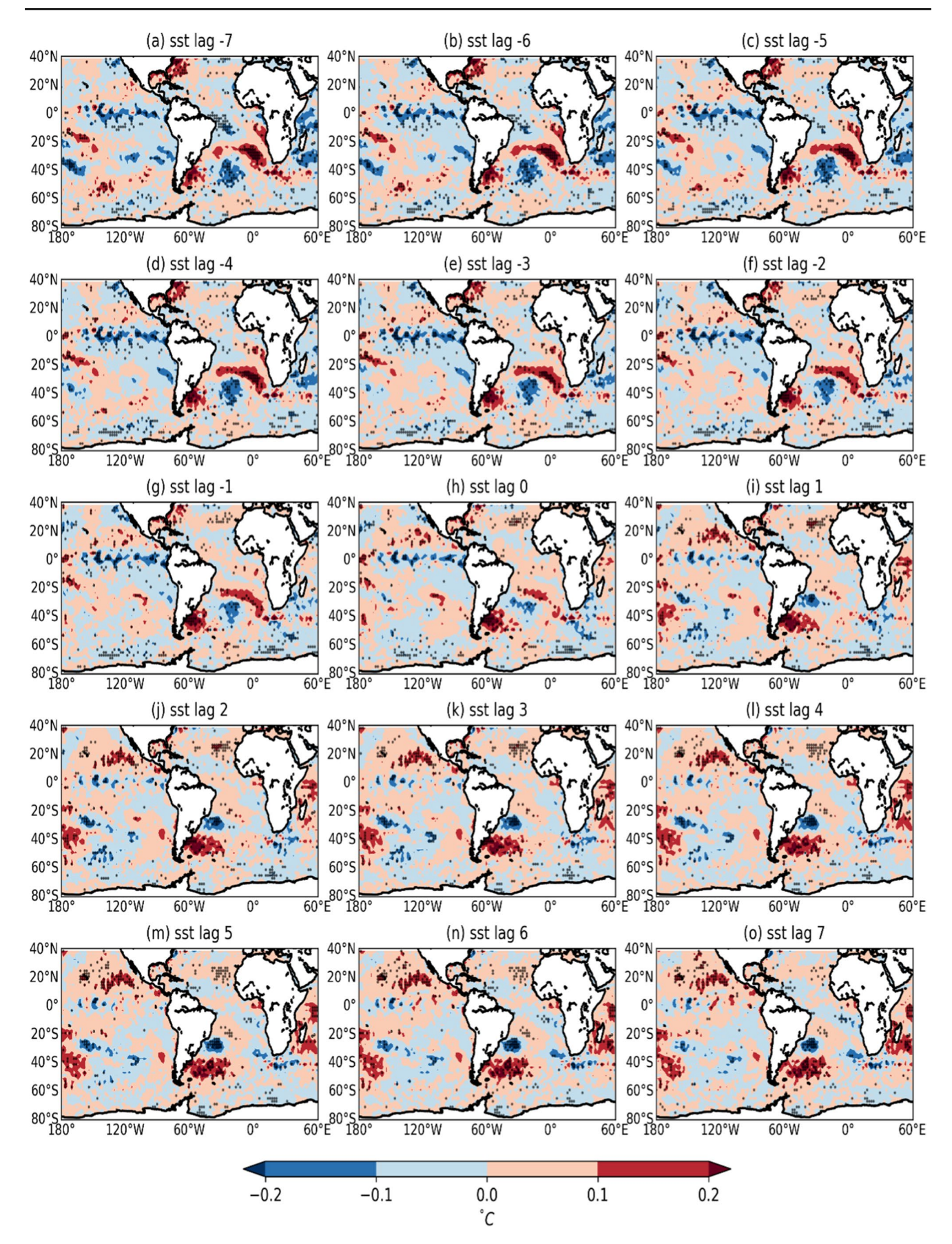
To answer these questions, we utilized two indices: the OMI (Kiladis et al. 2014) along with the criteria proposed by Jones et al. (2009) to define an MJO, and the daily RMM index (Wheeler and Hendon 2004) (see details in Section 2). Using these indices, we found that approximately 68% (75%) of the 32 persistent SACZ events were related to an active MJO based on the OMI (RMM) index. To further explore these results, we calculated the percentage of days during each SACZ event that were associated with an active MJO, independently of the duration of the event (Fig. 10). For example, if a SACZ event persisted for 10 days (or 8 days) with an active MJO during 5 (or 4 days) within that period, the fraction of days with an active MJO was equal to 50%. Figure 10 ordinate indicates the percentage of the 32 events that were observed in each category interval indicated in the abscissa. Using the OMI index and the Jones (2009) approach, the MJO was not considered active in 31% of these events (10 SACZs). Conversely, the MJO was active during the entire period characterized as a persistent SACZ in 56%

of the events (18 SACZs). When employing the RMM daily index and considering the RMM amplitude greater than 1.0 as the single criteria to define an active MJO, the MJO was active during the entire event in only 28% of the SACZs (9 SACZs). On the other hand, the number of events associated with an inactive MJO decreased to 25% (8 SACZs). These results exemplify the fact that the RMM daily index exhibits much higher fluctuations in amplitude than the OMI index (not shown). The implication of this fluctuation is an increase in the probability of an active MJO being observed during any SACZ event compensated by a decrease in the probability of a more consistent MJO signal during an event. The OMI index and the Jones (2009) methodology revealed that more than half of the SACZ events that have been associated with an active MJO maintained this association throughout the entire period these events persisted. These results clearly indicate the importance of monitoring the MJO activity to forecast the SACZ activity.

We also investigated the relationships between the MJO phase and the SACZ when the MJO was considered active (Fig. 11). Two aspects are worth noticing in these analyses. First, the canonical EOF projections on convection (OLR or precipitation) associated with these MJO indices in the study of Kiladis et al. (2014) and Wheeler and Hendon (2004) were obtained without considering seasonality and for much longer periods. The SACZ events discussed here were obtained over 18 years and were predominantly observed in January and February (Fig. 1), thus exhibited strong seasonality. Secondly, as discussed by Kiladis et al. (2014), the RMM exhibits a phase difference with respect to the OMI, which is clearly noticed in Fig. 11. Surprisingly, when using the OMI, persistent SACZ events were primarily associated with the MJO phase 3 (Ph3) and phase 4 (Ph4), with a preference for phase 4. Persistent SACZs were less frequent during phase 6 (Ph6) and phase 7 (Ph7). Conversely, when employing the RMM index, persistent SACZ events were more frequent during phase 4 (Ph4) and phase 5 (Ph5), with a preference for phase 5, and were less frequent during phase 2 (Ph2). Nonetheless, notice that differences in the frequency of events per MJO phase are less pronounced for the RMM index than for the OMI, suggesting that a better characterization of the MJO cycle with an index that is less variable in time is important in separating phases.

Figure 12 illustrates the MJO teleconnections with the SACZ by showing GPCP precipitation anomalies with respect to the January–February climatology during phases 3–4 and 6–7 based on the OMI. The reason for focusing on January–February is that precipitation anomalies are seasonally dependent (not shown), and the largest majority of the SACZ events occurred during these 2 months. Composites were performed for all days during the period observed with an active MJO in each one of the considered phases (110 events during phase 3, 87 during phase 4, 62 events during







◄Fig. 9 Lag composites of SST intraseasonal anomalies (20–90 days) (°C) for SACZ_{4-days} events. Statistically significant regions (at 95% confidence level) are shown with stippled patterns

phase 6, and 77 during phase 7). Two patterns of precipitation anomalies emerged. In phase 3, we observe suppressed precipitation over Indonesia and increased precipitation over the date line associated with the enhancement of convection over eastern Brazil, in the climatological position of the SACZ. In phase 4, convection builds up over the Indian Ocean, while suppression is maintained over Indonesia. This pattern of teleconnection appeared associated with a clear enhancement of precipitation along the SACZ from the continent to the Subtropical Atlantic, but now with stronger activity south of the SACZ climatological position, remarkably over the state of Sao Paulo, Brazil.

5 Conclusions

The SACZ is a unique feature of the SAMS that influences the water supply for millions of people living in tropical South America. Persistent rains and the development of orographic convection often associated with the SACZ have been related to devastating floods and mudslides that took the lives of numerous people, destroyed property, and disrupted large communities in Brazil. Therefore, forecasting conditions conducive to the development of persistent SACZ events is critical to issuing timely alerts and planning evacuation strategies, increasing the resilience of vulnerable communities to rainfall-related disasters. The main objective of this study is to investigate the physical and dynamic characteristics of persistent SACZ events (persistence greater than 7 days) using meteorological variables commonly examined in operational forecasts. Here we evaluate patterns of anomalous circulation at 850 hPa and 200 hPa, OLR (as a proxy for convective activity), and SST. These variables are routinely evaluated in operational weather forecasting. All variables were band-filtered (20-90 days) to retain variability on subseasonal timescales. The band-filtering methodology allowed us to analyze patterns with less influence of transients on synoptic timescales.

This study examined thirty-two SACZ events (eighteen summers) with persistence greater than 7 days identified according to the criteria that are operationally adopted by CPTEC/INPE. We also contrasted mechanisms driving persistent events against mechanisms associated with more transient SACZ events (lasting 4 days).

We show that persistent SACZ events are more frequent during the peak of the South American Monsoon (January and February). Despite the relatively small sample size (18 seasons, 8 LN, 5 EN, and 5 neutral seasons), our results suggest that these events are likely more common during the

cold (LN) compared to the warm (EN) and neutral phases of ENSO. Although ENSO teleconnections with South American climate are complex, one possible mechanism explaining these teleconnections is the ENSO modulation of the SALLJ (Montini et al. 2019). Nevertheless, longer periods covering more decades would be recommended for a more robust statistical analysis and to explore mechanisms explaining the relationships between persistent SACZ and ENSO phases.

This study points out the following main features as relevant prognostic observations for the organization of persistent SACZ events 7 days in advance:

a) Development of a semi-stationary midlatitude wave train with equivalent barotropic structure in the extratropics organized approximately 7 days preceding the events.

This wave train exhibits a "wavenumber-3" characteristic across South America (from 180°W to 60°E), with a trough observed in midlatitudes over the eastern South Pacific (east of Chile). This wave train is evident in circulation anomalies at 850 hPa and 200 hPa, and geopotential height (not shown).

b) Presence of anomalous cyclonic circulation offshore of southeastern Brazil as part of the wave train.

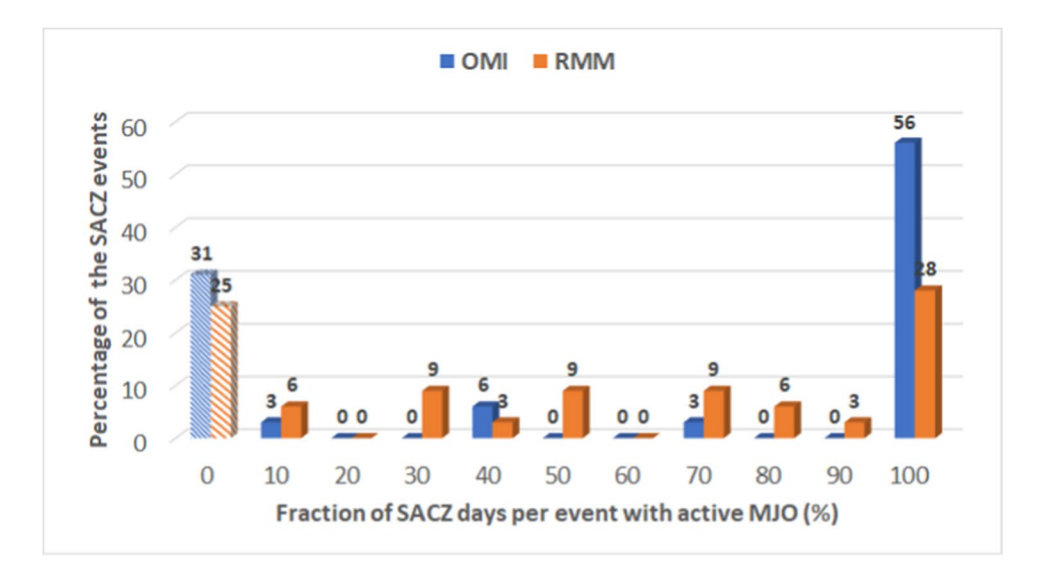
This anomalous cyclonic circulation is part of the wave train and induces the organization of an oceanic SACZ close to the southeastern coastal Brazil from lag -7 to lag -1. Contrastingly, shorter SACZ_{4-days} events are associated with a persistent cyclonic circulation far from the coast, approximately in the middle of the tropical Atlantic. The SACZ_{4-days} persistent cyclonic circulation organizes convection over the ocean from lag -5 to lag +2. Given the distance from the coast, the cyclonic feature does not significantly influence the enhancement of westerlies over tropical South America contrasting with persistent SACZ, which may explain the lack of thermodynamic support (moisture transport and convective instability) for extended SACZ periods.

c) Intensification of low-level westerlies over the continent induced by the offshore cyclonic anomaly.

The persistent cyclonic anomaly off the southeast coast of Brazil intensifies the oceanic SACZ from lag -7 to lag -1. Due to its position close to the continent, this cyclonic circulation induces low-tropospheric westerly winds over land. We hypothesize that these westerly winds advect moisture and convectively unstable air from the Amazon on the equatorward side of the SACZ. The impact of this enhanced transport is to increase moisture convergence and thus convection on the equatorward side of the SACZ, which results in the shift of the cyclonic circulation from the ocean to the continent on lag-0. We hypothesize that this shift is a critical factor in maintaining the continental SACZ active for long periods. Increased convection increase soil moisture,



Fig. 10 Percentage of SACZ events that were associated with an active MJO separated according to the respective fraction of days observed with an active MJO (indicated in the abscissa) according to the OMI (dark blue) and RMM (orange) indices. Stripped patterns indicate the respective fractions that were not associated with an active MJO



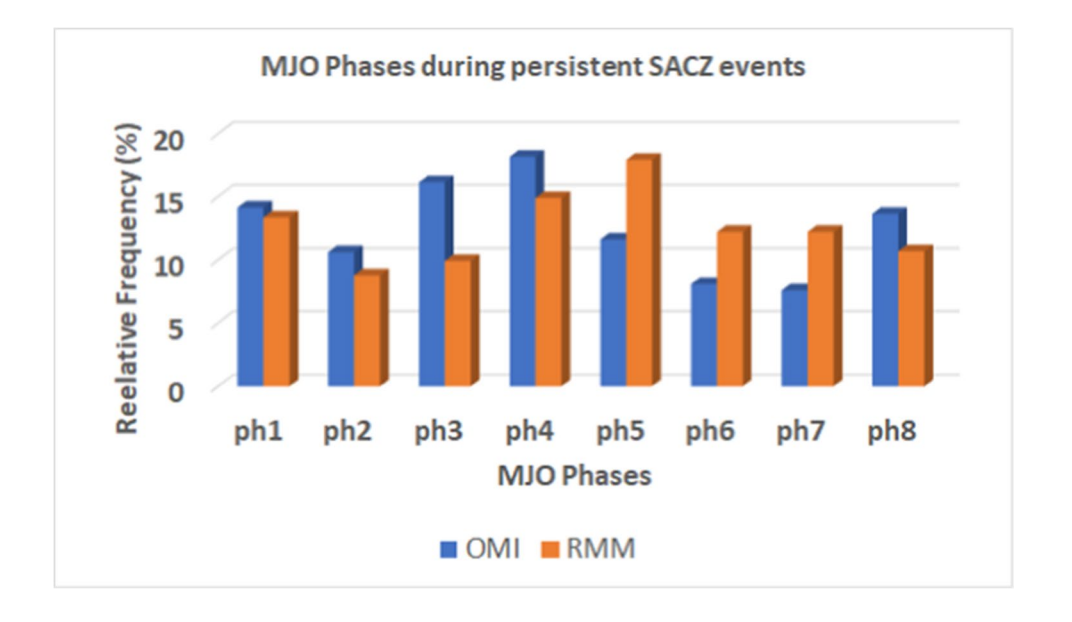
which in turn causes positive feedback for the maintenance of precipitation (Sorensson and Menéndez 2011). A similar continental shift of the oceanic cyclonic circulation is not observed for $SACZ_{4-days}$. Thus, $SACZ_{4-days}$ events appear to maintain their 'oceanic' component in lag-0.

- d) Amplification of the southern Pacific trough, evident from meridional (200 hPa) intraseasonal wind anomalies, from lag -7 to lag -1.
 - The amplification of the trough appears as a remarkable feature preceding persistent SACZ events. Thus, monitoring the intensification of meridional transports over the extratropical Pacific (east of the Chilean coast) can be useful in forecasting these events.
- e) Persistent upper-level (200 hPa) westerly (easterly) anomalies over tropical (subtropical) South America.

Our composites indicate that persistent 200 hPa westerly (easterly) intraseasonal anomalies over southeast Brazil (east Argentina) are important prognostic observations to infer that the wave train is active and to indicate where convection is becoming enhanced (suppressed).

f) Cold SST anomalies in the region of the Brazil-Malvinas Confluence (BMC) zone. Cold SST anomalies are perhaps among the most important prognostic variables concerning the probability of persistent SACZ events. Notice that cold anomalies can be observed more than 1 week prior to the occurrence of persistent SACZ. These maintenance and spatial extent of cold anomalies have been attributed to the coupling with low-level circulation anomalies caused by the near-shore cyclonic vortex preceding the continental SACZ.

Fig. 11 Frequency SACZ events that were associated with an active MJO separated according to the phase of the oscillation based on the OMI (blue) and RMM (orange) indices





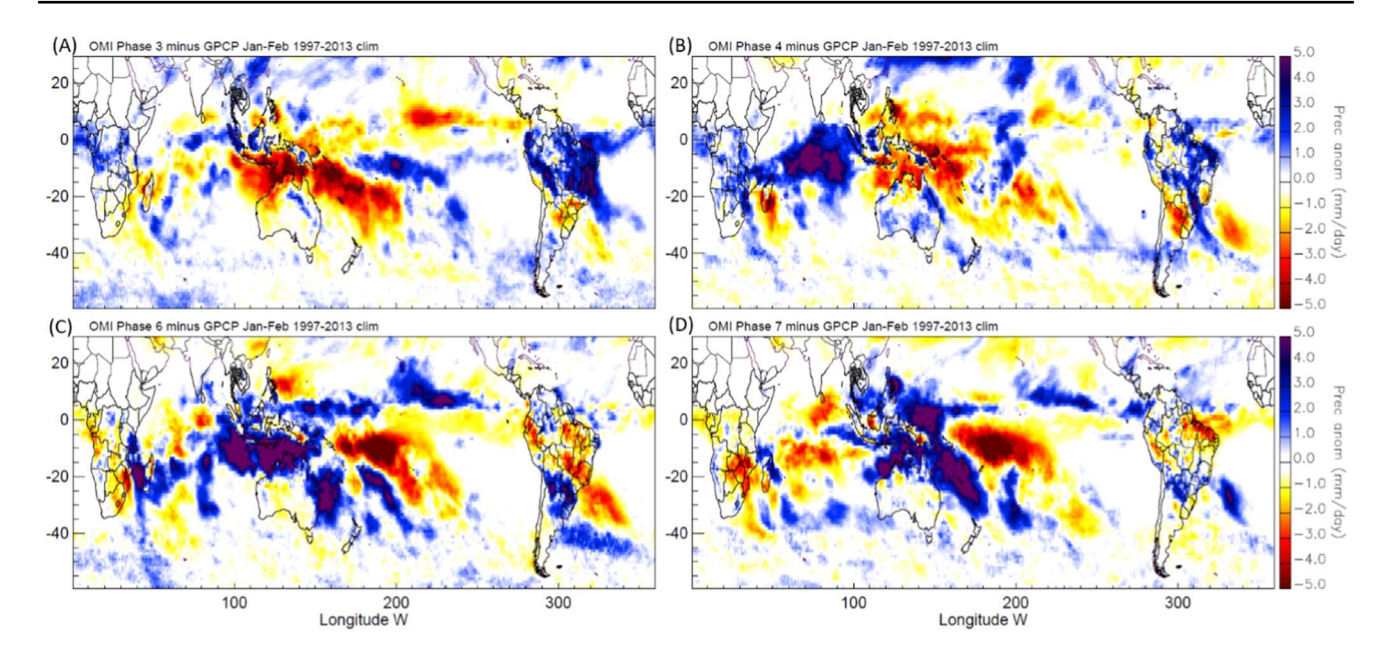


Fig. 12 Composites of GPCP precipitation anomalies with respect to the January–February climatology observed during (a) phase 3; (b) phase 4; (c) phase 6; (d) phase 7. Composites include MJO events

between January and February (1996–2013) obtained with OMI and characterized with Jones et al. (2009) methodology

These anomalies are dynamically driven by the winds and they change signal (from negative to positive) when the SACZ is active over the continent (lag-0) and for positive lags. Short SACZ_{4-days} events exhibit opposite behavior. Positive anomalies are observed persisting all lags along the BMC, possibly driven by persistent anticyclonic circulation south of the oceanic SACZ_{4-days}. We hypothesized that the anomalous cyclonic circulation observed over the central tropical Atlantic increases the transport of warmer water eastward and cold water westward, creating a distinct signature of SST anomalies over the tropical South Atlantic. These features support the dynamical nature of the atmospheric-ocean coupling on intraseasonal timescales (Pezzi et al. 2022).

Since the MJO is the most relevant mode of tropical teleconnection on intraseasonal timescales, we explored the relationships between the oscillation and persistent SACZ events based on the OMI and RMM daily indices. The main take away message from these analyses is that the MJO seems associated with the majority of persistent SACZ events, independently of the index. Therefore, appropriate monitoring of the MJO seems critical for forecasting these extreme events. However, some caveats need to be considered in these analyses. First, daily MJO indices need to be carefully examined. As pointed out by Jones et al. (2009), using simple criteria based on the amplitude of the index without considering the eastward propagation of the oscillation to decide whether the MJO is active may lead to false alarms and poor characterization of the

MJO cycle. Additionally, different indices may exhibit a difference in phases (Kiladis et al. 2014) that need to be carefully considered. Our study also suggests that the MJO teleconnections with the SACZ exhibit seasonality. According to the OMI index and using more restrictive criteria to define the MJO cycle, we show that persistent SACZs during January–February seem to occur more frequently during phases 3 and 4 and less frequently during phases 6 and 7.

Supplementary Information The online version contains supplementary material available at https://doi.org/10.1007/s00704-023-04375-7.

Acknowledgements The authors thank Dr. Luciano Pezzi for the fruitful discussions and Dr. Charles Jones for the important comments, suggestions, and algorithms for the characterization of the MJO cycle. Comments and suggestions from the anonymous reviewers were much appreciated.

Author contribution Wendell M. B. Fialho: conceptualization, methodology, formal analysis, validation, writing (original draft), visualization, and supervision. Leila M. V. Carvalho: conceptualization, methodology, formal analysis, writing, reviewing, editing, and supervision. Manoel A. Gan: formal analysis, writing, review, and editing. Sandro F. Veiga: validation, visualization, and computational support.

Funding This study was supported by the National Council for Scientific and Technological Development (CNPq) grant number 140710/2018–3. This work constitutes part of the first author's PhD dissertation at The National Institute for Space Research (INPE). Leila M. V. Carvalho received the National Science Foundation (NSF) AGS 1937899 support.

Data availability The NCEP/NCAR reanalysis for making the CFS data sets are at https://rda.ucar.edu/#!lfd?nb=y&b=proj&v=NCEP%20Cli



mate%20Forecast%20System%20Reanalysis. Climate Data Record Program data are available at https://www.ncei.noaa.gov/data/outgo ing-longwave-radiation-daily/access/. NOAA-Optimum Interpolation Sea Surface Temperature data are available at https://psl.noaa.gov/data/gridded/data.noaa.oisst.v2.highres.html. Climanalise Bulletin from CPTEC/INPE SACZ cases are available at http://climanalise.cptec.inpe.br/~rclimanl/boletim/. The OMI index was obtained at https://www.psl.noaa.gov/mjo/mjoindex/. The RMM index is available at http://www.bom.gov.au/climate/mjo/.

Code availability Code is available upon reasonable request.

Declarations

Ethics approval Not applicable.

Consent to participate Not applicable.

Consent for publication Not applicable.

Conflict for interest The authors declare no competing interests.

References

- Acevedo OC, Pezzi LP, Souza RB, Anabor V, Degrazia GA (2010) Atmospheric boundary layer adjustment to the synoptic cycle at the Brazil-Malvinas Confluence, South Atlantic Ocean. J Geophys Res: Atmos 115:1–12. https://doi.org/10.1029/2009JD013785
- Alcântara E, Marengo JA, Mantovani J, Londe L, San RLY, Park E, Lin YN, Mendes T, Cunha AP, Pampuch L, Seluchi M, Simões S, Cuartas LA, Massi K, Alvalá R, Moraes O, Filho CS, Mendes R, Nobre C (2022) Deadly disasters in Southeastern South America: flash floods and landslides of February 2022 in Petrópolis, Rio de Janeiro. Nat Hazards Earth Syst Sci [preprint]. https://doi.org/10. 5194/nhess-2022-163
- Ambrizzi T, Ferraz SET (2015) An objective criterion for determining the South Atlantic Convergence Zone. Front Environ Sci 3:1–9. https://doi.org/10.3389/fenvs.2015.00023
- Barcellos PCL, Silva FP, Vissirini FSB, Magalhães CA, Terra JM, Dutra MRF, Amaral ICF (2016) Diagnóstico meteorológico dos desastres naturais ocorridos nos últimos 20 anos na cidade de Duque de Caxias. Revista Brasileira de Meteorologia 31:319–329. https://doi.org/10.1590/0102-778631320150146
- Barreiro M, Chang P, Saravanan R (2002) Variability of the South Atlantic Convergence Zone simulated by an atmospheric general circulation model. J Clim 15:745–763. https://doi.org/10.1175/1520-0442(2002)015%3c0745:VOTSAC%3e2.0.CO;2
- Barreiro M, Chang P, Saravanan R (2005) Simulated precipitation response to SST forcing and potential predictability in the region of the South Atlantic Convergence Zone. Clim Dyn 24:105–114. https://doi.org/10.1007/s00382-004-0487-9
- Bombardi RJ, Carvalho LMV, Jones C (2014a) Simulating the influence of the South Atlantic dipole on the South Atlantic Convergence Zone during neutral ENSO. Theoret Appl Climatol 118:251–269. https://doi.org/10.1007/s00704-013-1056-0
- Bombardi RJ, Carvalho LMV, Jones C, Reboita MS (2014b) Precipitation over eastern South America and the South Atlantic sea surface temperature during neutral ENSO periods. Clim Dyn 42:1553–1568. https://doi.org/10.1007/s00382-013-1832-7
- Bueno Repinaldo HF, Nicolini M, Skabar YG (2015) Characterizing the diurnal cycle of low-level circulation and convergence using

- CFSR data in southeastern South America. J Appl Meteorol Climatol 54:671–690. https://doi.org/10.1175/JAMC-D-14-0114.1
- Carvalho LMV, Jones C, Liebmann B (2002a) Extreme precipitation events in southeastern South America and large-scale convective patterns in South Atlantic Convergence Zone. J Clim 15:2377–2395. https://doi.org/10.1175/1520-0442(2002)015%3c2377: EPEISS%3e2.0.CO;2
- Carvalho LMV, Silva Dias MAF (2021) Mesoscale and high impact weather in the South American monsoon. In: Chang CP, Ha KJ, Johnson RH, Kim D, Lau GNC, Wang B (eds) The multi-scale global monsoon system, 4th Edition. World Scientific Series on Asia-Pacific Weather and Climate. Vol. 11, World Scientific Publishing Company, Singapore, 500 pp., Chapter 12, p 151–160. https://doi.org/10.1142/9789811216602_0012
- Carvalho LMV, Jones C, Silva Dias MAF (2002b) Intraseasonal large-scale circulations and mesoscale convective activity in tropical South America during the TRMM-LBA campaign. J Geophys Res: Atmos 107:D20. https://doi.org/10.1029/2001J D000745
- Carvalho LMV, Jones C, Liebmann B (2004) The South Atlantic Convergence Zone: itensity, form, persistence and relationships with intraseasonal to interannual activity and extreme rainfall. J Clim 17:88–108. https://doi.org/10.1175/1520-0442(2004)017% 3c0088:TSACZI%3e2.0.CO;2
- Carvalho LMV, Silva AE, Jones C, Liebmann B, Silva Dias PL, Rocha HR (2011) Moisture transport and intraseasonal variability in the South America monsoon system. Clim Dyn 36:1865–1880. https://doi.org/10.1007/s00382-010-0806-2
- Carvalho LMV, Jones C, Posadas AND, Quiroz R, Bookhagen B, Liebmann B (2012) Precipitation characteristics of the South American Monsoon System Derived from multiple datasets. J Clim 25:4600–4620. https://doi.org/10.1175/JCLI-D-11-00335.1
- Chaves RR (2004) Nobre P (2004) Interactions between sea surface temperature over the South Atlantic Ocean and the South Atlantic Convergence Zone. Geophys Res Lett 31:L03204. https://doi.org/ 10.1029/2003GL018647
- Coelho CA, Oliveira CP, Ambrizzi T, Reboita MS, Carpenedo CB, Campos JLPS, Tomaziello ACN, Pampuch LA, Custódio MDS, Dutra LMM, Rocha RP (2016) The 2014 southeast Brazil austral summer drought: regional scale mechanisms and teleconnections. Clim Dyn 46:3737–3752. https://doi.org/10.1007/ s00382-015-2800-1
- Cunningham CAC, Cavalcanti IFA (2006) Intraseasonal modes of variability affecting the South Atlantic Convergence Zone. Int J Climatol 26:1165–1180. https://doi.org/10.1002/joc.1309
- De Almeida RAF, Nobre P, Haarsma RJ, Campos EJD (2007) Negative ocean-atmosphere feedback in the South Atlantic Convergence Zone. Geophys Res Lett 34:L18809. https://doi.org/10.1029/ 2007GL030401
- Doyle ME, Barros VR (2002) Midsummer low-level circulation and precipitation in subtropical South America and related sea surface temperature anomalies in the South Atlantic. J Clim 15:3395–3410. https://doi.org/10.1175/1520-0442(2002)015%3c3394: MLLCAP%3e2.0.CO;2
- Ferraz SET (2000) Oscilações intrasazonais no Sul e Sudeste do Brasil durante o verão. Dissertation, University of Sao Paulo
- Ferreira NJ, Sanches M, Silva Dias MAF (2004) Composição da zona de convergência do atlântico sul em períodos de El Niño e La Niña. Revista Brasileira de Meteorologia 19:98–98
- Gan MA, Kousky VE, Ropelewski CF (2004) The South America monsoon circulation and its relationship to rainfall over west-central Brazil. J Clim 17:47–66. https://doi.org/10.1175/1520-0442(2004) 017%3c0047:TSAMCA%3e2.0.CO;2
- Garcia SR, Kayano MT (2010) Some evidence on the relationship between the South American monsoon and the Atlantic ITCZ.



- Theoret Appl Climatol 99:29–38. https://doi.org/10.1007/s00704-009-0107-z
- Garcia SR, Kayano MT (2011) Moisture and heat budgets associated with the South American monsoon system and the Atlantic ITCZ. Int J Climatol 31:2154–2167, https://doi.org/10.1002/joc.2221
- Gelbrecht M, Boers N, Kurths J (2018) Phase coherence between precipitation in South America and Rossby waves. Sci Adv 4:1–9. https://doi.org/10.1126/sciadv.aau3191
- Gonzalez PLM, Vera CS (2014) Summer precipitation variability over South America on long and short intraseasonal timescales. Clim Dvn 43:1993–2007. https://doi.org/10.1007/s00382-013-2023-2
- Grimm AM (2019) Madden–Julian Oscillation impacts on South American summer monsoon season: precipitation anomalies, extreme events, teleconnections, and role in the MJO cycle. Clim Dyn 53:907–932. https://doi.org/10.1007/s00382-019-04622-6
- Grimm AM, Barros VR, Doyle ME (2000) Climate variability in Southern South America associated with El Niño and La Niña events. J Clim 13:35–58. https://doi.org/10.1175/1520-0442(2000) 013<0035:CVISSA>2.0.CO;2
- Grimm AM, Zilli MT (2009) Interannual variability and seasonal evolution of summer monsoon rainfall in South America. J Clim 22:2257–2275. https://doi.org/10.1175/2008JCLI2345.1
- Grimm AM, Hakoyama LR, Scheibe LA (2021) Active and break phases of the South American summer monsoon: MJO influence and subseasonal prediction. Clim Dyn 56:3603–3624. https://doi.org/10.1007/s00382-021-05658-3
- Herdies DL, Silva AD, Silva Dias MAF, Ferreira RN (2002) Moisture budget of the bimodal pattern of the summer circulation over South America. J Geophys Res: Atmos 107:8075. https://doi.org/10.1029/2001JD000997
- Hoskins BJ, Ambrizzi T (1993) Rossby wave propagation on a realistic longitudinally varying flow. J Atmos Sci 50:1661–1671. https://doi.org/10.1175/1520-0469(1993)050%3c1661:RWPOAR%3e2.0. CO:2
- Jones C (2016) The Madden-Julian oscillation and the monsoons. In: Carvalho LMV, Jones C (eds) The monsoons and climate change: observations and modeling. Springer International Publishing, Berlin, pp 207–221 (ISBN: 978-3-319-21650-8)
- Jones C (2009) A homogeneous stochastic model of the Madden– Julian oscillation. J of Clim 22:3270–3288. https://doi.org/10. 1175/2008JCLI2609.1
- Jones C, Carvalho LMV (2002) Active and break phases in the South American Monsoon System. J Clim 15:905–914. https://doi.org/ 10.1175/1520-0442(2002)015%3c0905:AABPIT%3e2.0.CO;2
- Jones C, Waliser DE, Gautier C (1998) The influence of the Madden-Julian oscillations on ocean surface heat fluxes and sea surface temperature. J Clim 11:1057–1072. https://doi.org/10.1175/ 1520-0442(1998)011%3c1057:TIOTMJ%3e2.0.CO;2
- Jorgetti T, Silva Dias PL, Freitas ED (2014) The relationship between South Atlantic SST and SACZ intensity and positioning. Clim Dyn 42:3077–3086. https://doi.org/10.1007/s00382-013-1998-z
- Kiladis GN, Dias J, Straub KH, Wheeler MC, Tulich SN, Kikuchi K, Weickmann KM, Ventrice MJ (2014) A comparison of OLR and circulation based indices for tracking the MJO. Mon Weather Rev 142:1697–1715. https://doi.org/10.1175/MWR-D-13-00301.1
- Kodama Y (1992) Large-scale features of subtropical precipitation zones (the baiu frontal zone, the SPCZ, and the SACZ) part I: characteristics of subtropical frontal zones. J Meteorol Soc Jpn 70:813–835. https://doi.org/10.2151/jmsj1965.70.4_813
- Kodama Y (1993) Large-scale features os subtropical precipitation zones (the baiu frontal zone, the SPCZ, and the SACZ) part II: conditions of circulations for generating the STCZs. J Meteorol Soc Jpn 71:581–610. https://doi.org/10.2151/jmsj1965.71.5 581
- Lafleur DM, Barrett BS, Henderson GR (2015) Some climatological aspects of the Madden–Julian Oscillation (MJO). J Clim 28:6039– 6053. https://doi.org/10.1175/JCLI-D-14-00744.1

- Lee HT, Heidinger A, Gruber A, Ellingson RG (2004) The HIRS outgoing longwave radiation product from hybrid polar and geosynchronous satellite observations. Adv Space Res 33:1120–1124. https://doi.org/10.1016/S0273-1177(03)00750-6
- Liebmann B, Jones C, Carvalho LMV (2001) Interannual variability of daily extreme precipitation events in the State of São Paulo, Brazil. J Clim 14:208–218. https://doi.org/10.1175/1520-0442(2001) 014%3c0208:IVODEP%3e2.0.CO;2
- Liebmann B, Kiladis GN, Marengo JA, Ambrizzi T, Glick JD (1999) Submonthly convective variability over South America and South Atlantic Convergence Zone. J Clim 12:1877–1891. https://doi.org/ 10.1175/1520-0442(1999)012%3c1877;SCVOSA%3e2.0.CO;2
- Liebmann B, Kiladis GN, Vera CS, Saulo AC, Carvalho LMV (2004)
 Subseasonal variations of rainfall in South America in the vicinity of the low-level jet east of the Andes and comparison to those in the South Atlantic Convergence Zone. J Clim 17:3829–3842. https://doi.org/10.1175/1520-0442(2004)017%3c3829:SVORIS%3e2.0 CO:2
- Madden RA, Julian PR (1994) Observations of the 40–50 day tropical oscillation: a review. Mon Weather Rev 122:1994. https://doi.org/10.1175/1520-0493(1994)122%3c0814:OOTDTO%3e2.0.CO;2
- Marengo JA, Jones R, Alves LM, Valverde MC (2009) Future change of temperature and precipitation extremes in South America as derived from the PRECIS regional climate modeling system. Int J Climatol 29:2241–2255. https://doi.org/10.1002/joc.1863
- Mo KC, Higgins RW (1998) The Pacific-South American modes and tropical convection during the southern hemisphere winter. Mon Weather Rev 126:1581–1596. https://doi.org/10.1175/ 1520-0493(1998)126%3c1581:TPSAMA%3e2.0.CO;2
- Montini TL, Jones C, Carvalho LMV (2019) The South American low-level jet: a new climatology, variability, and changes. J Geophys Res: Atmos 124:1200–1218. https://doi.org/10.1029/2018JD029634
- Muza MN, Carvalho LMV, Jones C, Liebmann B (2009) Intraseasonal and interannual variability of extreme dry and wet events over southeastern South America and the subtropical Atlantic during austral summer. J Clim 22:1682–1699. https://doi.org/10.1175/2008JCLI2257.1
- Neelin JD, Held IM (1987) Modeling tropical convergence based on the moist static energy budget. Mon Weather Rev 115:3–12. https://doi.org/10.1175/15200493(1987)115%3c0003: MTCBOT%3e2.0.CO;2
- Nieto-Ferreira R, Rickenbach TM, Herdies DL, Carvalho LMV (2003) Variability of South American convective cloud systems and tropospheric circulation during January–March 1998 and 1999. Mon Weather Rev 131:961–973. https://doi.org/10.1175/1520-0493(2003)131%3c0961:VOSACC%3e2.0.CO;2
- Nobre CA, Marengo JA, Seluchi ME, Cuartas LA, Alves LM (2016) Some characteristics and impacts of the drought and water crisis in Southeastern Brazil during 2014 and 2015. J Water Resour Prot 8:252–262. https://doi.org/10.4236/jwarp.2016.82022
- Nobre P, De Almeida RA, Malagutti M, Giarolla E (2012) Coupledatmosphere variations over the South Atlantic. J Clim 25:6349– 6358. https://doi.org/10.1175/JCLI-D-11-00444.1
- Nogués-Paegle J, Mo KC (1997) Alternating wet and dry conditions over South America during summer. Mon Weather Rev 125:279–291. https://doi.org/10.1175/1520-0493(1997)125%3c0279: AWADCO%3e2.0.CO;2
- Nogués-Paegle J, Byerle LA, Mo KC (2000) Intraseasonal modulation of South American summer precipitation. Mon Weather Rev 128:837–850. https://doi.org/10.1175/1520-0493(2000)128% 3c0837:IMOSAS%3e2.0.CO;2
- Petersen WA, Nesbitt SW, Blakeslee RJ, Cifelli R, Hein P, Rutledge SA (2002) TRMM observations of intraseasonal variability in convective regimes over the Amazon. J Clim 15:1278–1294. https://doi.org/10.1175/1520-0442(2002)015%3c1278:TOOIVI%3e2.0.CO;2



- Peterson RG, Stramma L (1991) Upper-level circulation in the South Atlantic Ocean. Prog Oceanogr 26:1–73. https://doi.org/10.1016/0079-6611(91)90006-8
- Pezzi LP, Souza RB, Dourado MS, Garcia CAE, Mata MM, Silva Dias MAF (2005) Ocean-atmosphere in situ observations at the Brazil-Malvinas Confluence region. Geophys Res Lett 32:1–4. https:// doi.org/10.1029/2005GL023866
- Pezzi LPP, Quadro MFL, Lorenzetti JA, Miller A, Rosa E, Lima L, Sutil U (2022) The effect of Oceanic South Atlantic Convergence Zone episodes on regional SST anomalies: the roles of heat fluxes and upper-ocean dynamics. Clim Dyn. https://doi.org/10.1007/ s00382-022-06195-3
- Quadro MFL (1994) Estudo de episódios de Zona de Convergência do Atlântico Sul (ZCAS) sobre a América do Sul. Dissertation, The National Institute for Space Research
- Quadro MFL, Silva Dias MAF, Herdies DL, Gonçalves LGG (2012) Análise climatológica da precipitação e do transporte de umidade na região da ZCAS através da nova geração de reanálises. Revista Brasileira de Meteorologia 27:152–162. https://doi.org/10.1590/ S0102-77862012000200004
- Reynolds RW, Smith TM, Liu C, Chelton DB, Casey KS, Schlax MG (2007) Daily high-resolution-blended analyses for sea surface temperature. J Clim 20:5473–5496. https://doi.org/10.1175/2007J CLJ1824.1
- Rickenbach TM, Ferreira RN, Halverson, JB, Herdies DL, Silva Dias MAF (2002) Modulation of convection in the southwestern Amazon basin by extratropical stationary fronts. Journal of Geophysical Research: Atmospheres 107(D20). https://doi.org/10.1029/2000JD000263
- Rodrigues RR, Taschetto AS, Gupta AS, Foltz GR (2019) Common cause for severe droughts in South America and marine heatwaves in the South Atlantic. Nat Geosci 12:620–626. https://doi.org/10.1038/s41561-019-0393-8
- Saha S, Moorthi S, Pan HL, Wu X, Wang J, Nadiga S, Tripp P, Kistler R, Woollen J, Behringer D, Liu H, Stokes D, Grumbine R, Gayno G, Wang J, Hou YT, Chuang HY, Juang H, Sela J, Iredell M, Treadon R, Kleist D, Delst PV, Keyser D, Derber J, Ek M, Meng J, Wei H, Yang R, Lord S, Dool HVD, Kumar A, Wang W, Long C, Chelliah M, Xue Y, Huang B, Schemm JK, Ebisuzaki W, Lin R, Xie P, Chen M, Zhou S, Higgins W, Zou CZ, Liu Q, Chen Y, Han Y, Cucurull L, Reynolds RW, Rutledge G, Goldberg M (2010) The NCEP climate forecast system reanalysis. Bull Am Meteor Soc 91:1015–1057. https://doi.org/10.1175/2010BAMS3001.1
- Sanches MB (2002) Análise sinótica da Zona de Convergência do Atlântico Sul (ZCAS) utilizando-se a técnica de composição. Dissertation, The National Institute for Space Research
- Schiro KA, Neelin JD, Adams DK, Lintner BR (2016) Deep convection and column water vapor over tropical land versus tropical ocean: a comparison between the Amazon and the tropical western Pacific. J Atmos Sci 73:4043–4063. https://doi.org/10.1175/JAS-D-16-0119.1
- Silva AE, Carvalho LMV (2007) Large-scale index for South America monsoon (LISAM). Atmos Sci Lett 8:51–57. https://doi.org/10. 1002/asl.150
- Sorensson AA, Menéndez CG (2011) Summer soil-precipitation coupling in South America. Tellus A: Dyn Meteorol Oceanogr 63A:56–68. https://doi.org/10.1111/j.1600-0870.2010.00468.x

- Spiegel MR, Stephens LJ (1999) Theory and problems of statistics. McGraw-Hill, New York
- Tao WK, Lang S, Olson WS, Meneghini R, Yang S, Simpson J, Kummerow C, Smith E, Halverson J (2001) Retrieved vertical profiles of latent heat release using TRMM rainfall products for February 1998. J Appl Meteorol Climatol 40:957–982. https://doi.org/10.1175/1520-0450(2001)040%3c0957:RVPOLH%3e2.0.CO;2
- Tedeschi RG, Grimm AM, Cavalcanti IFA (2015) Influence of Central and East ENSO on extreme events of precipitation in South America during austral spring and summer. Int J Climatol 35:2045–2064. https://doi.org/10.1002/joc.4106
- Tirabassi G, Masoller C, Barreiro M (2015) A study of the air–sea interaction in the South Atlantic Convergence Zone through Granger causality. Int J Climatol 35:3440–3453. https://doi.org/10.1002/joc.4218
- Tomaziello ACN, Carvalho LMV, Gandu AW (2016) Intraseasonal variability of the Atlantic Intertropical Convergence Zone during austral summer and winter. Clim Dyn 47:1717–1733. https://doi.org/10.1007/s00382-015-2929-y
- Vasconcelos Junior FC, Jones C, Gandu AW (2018) Interannual and intraseasonal variations of the onset and demise of the pre-wet season and the wet season in the Northern Northeast Brazil. Revista Brasileira de Meteorologia 33:472–484. https://doi.org/ 10.1590/0102-7786333007
- Vera C, Higgins W, Amador J, Ambrizzi T, Garreaud R, Gochis D, Gutzler D, Lettenmaier D, Marengo J, Mechoso CR, Nogués-Paegle J, Silva Dias PL, Zhang C (2006) Toward a unified view of the American Monsoon Systems. J Clim 19:4977–5000. https:// doi.org/10.1175/JCLI3896.1
- Vera CS, Alvarez MS, Gonzalez PLM, Liebmann B, Kiladis GN (2018) Seasonal cycle of precipitation variability in South America on intraseasonal timescales. Clim Dyn 51:1991–2001. https://doi.org/ 10.1007/s00382-017-3994-1
- Wheeler MC, Hendon HH (2004) An all-season real-time multivariate MJO index: development of an index for monitoring and prediction. Mon Weather Rev 132:1917–1932. https://doi.org/10.1175/ 1520-0493(2004)132%3c1917:AARMMI%3e2.0.CO;2
- Zilli M, Hart N (2021) Large-scale circulation changes over South America are impacting synoptic-scale tropical-extratropical interactions and altering rainfall seasonality. In Proceedings of the EGU General Assembly Conference, Viena, Austria, April 2021; pp. EGU21–10393. https://doi.org/10.5194/egusphere-egu21-10393
- Zilli MT, Carvalho LMV, Lintner BR (2019) The poleward shift of South Atlantic Convergence Zone in recent decades. Clim Dyn 52:2545–2563. https://doi.org/10.1007/s00382-018-4277-1

Publisher's note Springer Nature remains neutral with regard to jurisdictional claims in published maps and institutional affiliations.

Springer Nature or its licensor (e.g. a society or other partner) holds exclusive rights to this article under a publishing agreement with the author(s) or other rightsholder(s); author self-archiving of the accepted manuscript version of this article is solely governed by the terms of such publishing agreement and applicable law.

